

## END-SEMESTER REPORT



### CAPSTONE PROJECT (CP302)

Date of submission: 08/05/2024

*Supervised by*

**Dr. Anupam Agrawal**

*Submitted by*

Name	Entry Number
Aditya Kumar	2022MEB1290
Aryan Daga	2022MEB1300
Priyanshu Rao	2022MEB1331
Priyanshu Singh	2022MEB1332

**Department of Mechanical Engineering  
Indian Institute of Technology, Ropar**

## Table of Contents

---

Chapter / Section	Page
<b>Chapter 1. Title of the Project</b>	6
<b>Chapter 2. Introduction</b>	6
<b>Chapter 3. Literature Review</b>	7
3.1 Challenges in Ti <sub>6</sub> Al <sub>4</sub> V Forming	
3.2 Heat-Assisted ISF Techniques	
3.2.1 Global Heating Methods	
3.2.2 Localized Heating (Laser, Induction)	
3.2.3 Friction-Assisted Heating	
3.3 Numerical Modelling in ISF	
<b>Chapter 4. Current Solutions</b>	8
4.1 Traditional Forming Methods	
4.1.1 Hot Stamping	
4.1.2 Superplastic Forming	
4.1.3 Conventional ISF	
4.2 Advanced ISF Systems	
4.2.1 Laser-Assisted ISF	
4.2.2 Induction Heating SPIF	
4.2.3 Electric Hot ISF	
4.2.4 Friction Stir-Assisted ISF	
<b>Chapter 5. Objective</b>	10
5.1 Parameter Space Exploration	
5.2 Temperature-Dependent Behavior	
Characterization	
5.3 Stress and Process Mechanics Analysis	
5.4 Thickness Variation Analysis	

5.5 Simulation Methodology Refinement

**Chapter 6. Experimental and Analytical Details** 11

6.1 Material Properties and Specimen Description

6.2 Simulation Setup and Methodology

6.2.1 Specimen Geometry & Boundary Conditions

6.2.2 Tool Design & Trajectory Generation

6.2.2.1 Tool Design in SolidWorks

6.2.2.2 G-Code Generation in Fusion 360

6.2.2.3 Abaqus Integration (Amplitude Definition)

6.2.3 Numerical Simulation Configuration

6.3 Advanced Simulation Matrix

6.4 Results and Discussion

**Chapter 7. Work Done and Future Plans** 31

7.1 Work Completed

7.1.1 Integrated Process Development

7.1.2 Key Computational Outcomes

7.2 Future Work

7.2.1 Advanced Simulation Development

7.2.2 Physical Apparatus Development

7.2.3 Process Optimization

7.2.4 Validation Framework

**Chapter 8. Conclusion and Discussion** 33

8.1 Summary of Key Findings

8.2 Comparison with Literature

8.3 Implications for Process Design

8.4 Limitations

8.5 Recommendations for Future Work

**Chapter 9. References** 35

## Acknowledgment

---

We express our deepest and sincerest gratitude to Dr. Anupam Agrawal, our esteemed project advisor, whose expert insights, unwavering support, and dedicated guidance have been indispensable to the success of our development project.

We are profoundly grateful to our parents for providing us with the opportunity to pursue our ambitions and for their constant encouragement, which has served as a steadfast source of inspiration throughout our journey.

We extend our heartfelt appreciation to the distinguished researchers and scholars whose seminal works have significantly influenced and enriched our project. We also wish to acknowledge the collaborative spirit and invaluable contributions of our fellow mechanical engineering colleagues.

Lastly, we thank everyone who has played a role in advancing this project. With profound gratitude to the Almighty, we reflect on our collective journey with humility and eagerly anticipate further accomplishments in the future.

## Abstract

---

Incremental sheet forming (ISF) is a flexible dieless process that bends sheet metal via localized tool displacements, offering high geometric accuracy for complex parts but limited by material ductility at ambient temperatures. For high-strength Ti<sub>6</sub>Al<sub>4</sub>V, poor room-temperature formability leads to early tool lift-off and excessive thinning. Heat-assisted ISF (HA-ISF) mitigates these issues by thermally softening the sheet, reducing flow stress and springback

In this study, six explicit-dynamic finite-element simulations were conducted in Abaqus/Explicit using Johnson–Cook parameters at 25 °C and 600 °C to quantify the effects of temperature, wall angle, and forming depth on Ti<sub>6</sub>Al<sub>4</sub>V formability. Toolpaths were generated via a spiral strategy in Fusion 360 and imported into simulations as time-based amplitudes.

Key results show that at 600 °C full target depths (59.5 mm, 69.5 mm) are achieved with uniform minimum thickness  $\approx 0.50$  mm, compared to only  $\sim 39.3$  mm depth and severe thinning ( $\sim 0.35$  mm) at 25 °C. Von Mises stress is reduced by  $\approx 56\%$  under heat assistance, while wall-angle increases ( $45^\circ \rightarrow 60^\circ$ ) cause only a 6% stress rise at elevated temperature. Depth increases (59.5  $\rightarrow$  69.5 mm) at room temperature raise stress by  $\sim 3.7\%$ .

These findings confirm that pre-heating to 600 °C is essential for deep-wall ISF of Ti<sub>6</sub>Al<sub>4</sub>V and that the sine-law accurately predicts thickness under thermal softening. The workflow and results provide guidelines for industrial HA-ISF design, highlighting the need for localized heating strategies and refined simulation-experimental integration

## Chapter 1. Title of the Project

# Heat Assisted Incremental Sheet Metal Forming for Ti<sub>6</sub>Al<sub>4</sub>V

## Chapter 2. Introduction

Incremental Sheet Forming (ISF) is a dieless manufacturing process that gradually deforms sheet metal using a computer-controlled tool. Unlike conventional stamping or forming techniques, ISF uses a series of small, localized deformations to produce complex shapes without the need for dedicated dies. Although this technique has been successfully applied to ductile materials like aluminium, its use for high-strength alloys such as Ti<sub>6</sub>Al<sub>4</sub>V is limited by the alloy's poor formability at ambient conditions.

Ti<sub>6</sub>Al<sub>4</sub>V, a widely used titanium alloy in aerospace, biomedical, and automotive applications, exhibits a high yield strength (approximately 900 MPa) and low ductility (around 10% elongation) at room temperature. This inherent rigidity poses significant challenges when attempting to achieve the large plastic deformations required in forming processes. **Heat-Assisted Incremental Sheet Forming (HA-ISF)** overcomes these limitations by preheating the workpiece—thereby lowering the material's yield stress, reducing springback, and allowing for deeper draws. Heating not only enhances ductility but also minimizes the forces required for forming, thus enabling the fabrication of components with complex geometries and reduced risk of fracture.

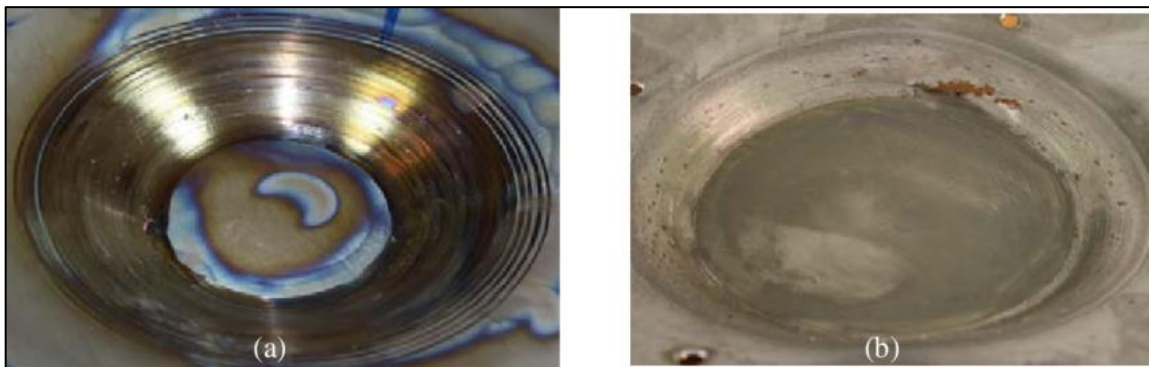


*Fig. 2.1: Sample Result of Incremental Sheet Forming (ISF)*

In the present study, the focus is on analyzing the thermomechanical behavior of Ti<sub>6</sub>Al<sub>4</sub>V during HA-ISF using finite element simulations performed in Abaqus. The work encompasses simulation studies that examine:

- Temperature-dependent flow stress reduction at elevated temperatures 600°C

- Incremental forming simulations using a conical tool path generated via CAD/CAM integration.

A detailed analysis of the material's behavior under both mechanical and thermal loads is provided, alongside a discussion on future experimental validation using a prototype HA-ISF apparatus. The workpiece for this study is a Ti<sub>6</sub>Al<sub>4</sub>V plate with dimensions 150 mm × 150 mm and a thickness of 1 mm. An 80 mm × 80 mm area is designated for the forming operation, while the remainder of the plate serves as the clamping zone.

## Chapter 3. Literature Review

---

### 3.1 Challenges in Ti<sub>6</sub>Al<sub>4</sub>V Forming

Ti<sub>6</sub>Al<sub>4</sub>V is a dual-phase ( $\alpha+\beta$ ) titanium alloy characterized by its high strength-to-weight ratio and excellent corrosion resistance. However, its limited ductility at room temperature is a major challenge in forming processes. The alloy's microstructure contributes to its high yield strength but also results in early onset of plastic instability when subjected to large deformations. Researchers have documented that dynamic recovery and recrystallization occur at elevated temperatures (typically between 300°C and 700°C), which reduce flow stress by up to 55% [1]. For example, Li et al. (2022) demonstrated that induction heating to 600°C can improve the formability of Ti<sub>6</sub>Al<sub>4</sub>V by approximately 40% compared to its room-temperature behavior [2].

### 3.2 Heat-Assisted ISF Techniques

To overcome the challenges posed by the low formability of Ti<sub>6</sub>Al<sub>4</sub>V, several heat-assisted ISF techniques have been explored:

- **Global Heating:**

The entire sheet is uniformly heated using furnaces or radiant heaters. While this method is straightforward, it may result in thermal gradients that cause non-uniform deformation.

- **Local Heating:**

Techniques such as laser or induction heating focus thermal energy on the immediate area of contact between the tool and the sheet. This approach reduces energy consumption and minimizes thermal effects on the clamped regions.

**Friction-Assisted Heating:**

In this variant, heat is generated by friction between the forming tool and the sheet. The inherent heat produced during tool rotation can eliminate the need for an external heat source.

Key literature findings include:

- The optimal forming temperature for Ti<sub>6</sub>Al<sub>4</sub>V typically ranges between 500°C and 700°C [3].
- Toolpath optimization is essential to minimize geometric inaccuracies arising from thermal expansion.
- Appropriate lubricants, such as graphite or MoS<sub>2</sub>, are used to reduce tool wear and prevent adhesion of the titanium alloy to the forming tool.

### 3.3 Numerical Modelling in ISF

Numerical simulation plays a crucial role in predicting the outcomes of incremental forming processes. The Finite Element Method (FEM) is widely used to simulate complex forming operations. In the context of HA-ISF, FEM simulations must account for both the mechanical deformation and the thermal effects. One of the most commonly used material models for such analyses is the **Johnson-Cook plasticity model**, which captures the temperature- and strain-rate-dependent behavior of metals. The Johnson-Cook model is expressed as:

$$Y = [A + B\varepsilon_p^n] [1 + C \ln \varepsilon_p^*] [1 - T_H^m]$$

where

$\varepsilon_p$  = effective plastic strain

$\varepsilon_p^*$  = normalized effective plastic strain rate

$T_H$  = homologous temperature =  $(T - T_{\text{room}}) / (T_{\text{melt}} - T_{\text{room}})$

## Chapter 4. Current Solutions

### 4.1 Traditional Forming Methods

Traditional forming processes for titanium alloys include:

#### 1. Hot Stamping:

This traditional technique involves preheating titanium sheets before forming them between matched dies. While effective for basic geometries, hot stamping presents several limitations:

- High tooling costs for complex components
- Significant energy consumption for global heating
- Long cycle times due to heating and cooling requirements



2. **Superplastic Forming:**

This specialized process exploits titanium's superplastic behavior at elevated temperatures (typically 900°C) and low strain rates ( $10^{-5}$  to  $10^{-4}$  s<sup>-1</sup>).

According to the search results, SPF offers excellent formability but requires specific grain sizes and extremely long cycle times, making it economically viable only for high-value components.

3. **Conventional Incremental Forming:** At room temperature, standard ISF techniques show limited effectiveness for Ti<sub>6</sub>Al<sub>4</sub>V. Experimental studies indicate that the minimum major strain achievable for Ti<sub>6</sub>Al<sub>4</sub>V alloy sheet using conventional hydroforming at room temperature ranges from 0.15 to 0.25, substantially lower than what is possible with more ductile materials.

## 4.2 Advanced ISF Systems

In recent years, several advanced systems have been developed for incremental forming:

1. **Laser-Assisted ISF:**

This approach uses laser heating to create a localized hot zone ahead of the forming tool. Research indicates that this method:

- Reduces forming forces by up to 40%
- Improves dimensional accuracy
- Enables steeper wall angles

However, challenges include high equipment costs and precise synchronization requirements between laser positioning and tool movement.

2. **Induction Heating:**

Li's 2022 research developed an induction heating SPIF system capable of processing Ti<sub>6</sub>Al<sub>4</sub>V sheets at temperatures of 600°C and 700°C. Results demonstrated:

- Significant improvement in formability
- More uniform thickness distribution
- Reduced springback effects

The main limitation involves controlling the heating zone size and maintaining uniform temperature distribution.

3. **Electric Hot Incremental Forming (EHIF):** This technique applies electric current directly through the tool-sheet interface to generate resistance heating. A 2019 study showed that EHIF could improve the formability of Ti<sub>6</sub>Al<sub>4</sub>V while producing more uniform thickness distribution compared to cold forming.

4. **Friction Stir-Assisted ISF:** Golakiya and Chudasama's 2022 research demonstrated that friction-generated heat could significantly enhance the formability of Ti<sub>6</sub>Al<sub>4</sub>V sheets. Their approach eliminated the need for external heating sources but introduced challenges related to tool wear and process control.

Despite these innovations, challenges remain:

- **Thermal Gradient Management:** Uneven temperature distribution across the forming zone leads to non-uniform deformation and residual stresses. Current research has not fully addressed optimal heating strategies to minimize these effects for complex titanium components.
- **Tool-Material Interaction at Elevated Temperatures:** Ti<sub>6</sub>Al<sub>4</sub>V exhibits a strong tendency for adhesion to tooling above 400°C. According to search results, this leads to accelerated tool wear and surface quality issues.
- **Process Parameter Optimization:** While individual parameters have been studied, systematic optimization of the complete parameter space (temperature, tool path, step size, etc.) for Ti<sub>6</sub>Al<sub>4</sub>V in heat-assisted ISF is not well established.
- **Energy Efficiency Considerations:** Duflou's research indicates that ISF processes consume between 610 and 740 Watts on average. However, comprehensive energy efficiency analyses comparing different heating strategies for titanium forming are lacking.
- **Simulation-Experimental Correlation:** Validation studies correlating advanced simulation models with experimental results, particularly for complex geometries and multi-stage forming operations in heated conditions, remain limited.

## Chapter 5. Objective

---

The primary objectives of this project are:

### 5.1 Comprehensive Parameter Space Exploration

- Systematically analyze the effects of wall angle (20°, 45°, and 60°), forming depth (9.5-69.5 mm), step-over distance (0.25-0.5 mm), and mass scaling factors on formability outcomes
- Establish optimal parameter combinations for maximizing formability while minimizing defects.

## 5.2 Temperature-Dependent Material Behavior Characterization

- Quantify the reduction in yield stress and flow stress of Ti<sub>6</sub>Al<sub>4</sub>V at 600°C compared to room temperature
- Evaluate the effectiveness of the Johnson-Cook plasticity and damage models in capturing temperature-dependent deformation and failure mechanisms
- Assess the impact of thermal conditions on thickness distribution and geometric accuracy

## 5.3 Process Mechanics and Stress Analysis

- Analyze stress distributions (Von Mises, principal) during incremental forming under different thermal conditions
- Identify critical stress states that lead to successful forming versus material failure
- Develop guidelines for stress-based process control in industrial applications

## 5.4 Thickness Variation Analysis

- Compare theoretical thickness predictions based on the sine law with simulation results across varying wall angles and depths
- Analyze thickness distribution patterns along the formed profile for all seven simulations
- Identify critical thinning zones and develop strategies to mitigate excessive thinning

## 5.5 Simulation Methodology Refinement

- Optimize mass scaling factors for balancing computational efficiency and simulation accuracy
- Develop efficient approaches for toolpath generation and integration into Abaqus simulations
- Establish best practices for thermomechanical coupling in explicit dynamic analyses

# Chapter 6. Experimental and Analytical Details

---

## 6.1 Material Properties and Specimen Description

1. This research focuses on Ti<sub>6</sub>Al<sub>4</sub>V (Grade 5) titanium alloy, a material widely used in aerospace, biomedical, and automotive applications due to its exceptional strength-to-weight ratio and corrosion resistance.
2. To accurately capture its temperature-dependent behavior, we implemented distinct material property sets for room temperature (25°C) and elevated temperature (600°C) conditions.

**Table 6.1: Temperature-Dependent Material Properties of Ti<sub>6</sub>Al<sub>4</sub>V**

Property	Room Temperature (25°C)	Elevated Temperature (600°C)
<b>Johnson-Cook Damage Parameters</b>		
d <sub>1</sub>	-0.09	-0.15
d <sub>2</sub>	0.25	0.4
d <sub>3</sub>	-0.5	-0.65
d <sub>4</sub>	0.014	0.01
d <sub>5</sub>	3.87	3
T <sub>melting</sub> (°C)	1604	1604
T <sub>transition</sub> (°C)	980	980
Reference strain rate	1	1
<b>Johnson-Cook Plasticity Parameters</b>		
A (MPa)	1000	620
B (MPa)	780	220
n	0.47	0.28
m	1.02	1
<b>Physical and Mechanical Properties</b>		
Mass density (tonne/mm <sup>3</sup> )	4.43 × 10 <sup>-9</sup>	4.43 × 10 <sup>-9</sup>
Young's modulus (GPa)	113.8	80
Poisson's ratio	0.34	0.34

These properties are critical for accurately modeling both the mechanical and thermal behavior of the alloy during simulation.

## 6.2 Simulation Setup and Methodology

### 6.2.1 Specimen Geometry and Boundary Conditions

The workpiece for all simulations consisted of a Ti<sub>6</sub>Al<sub>4</sub>V plate with the following specifications:

- Dimensions: 150 mm × 150 mm
- Thickness: 1 mm
- Exposed forming area: 80 mm × 80 mm (central region)
- Boundary conditions: Fixed displacement (clamped) along the periphery outside the forming area

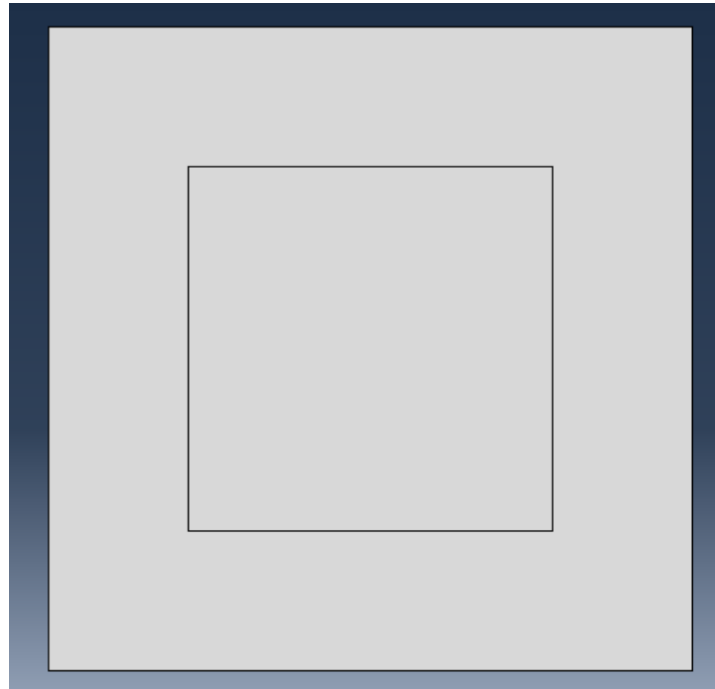


*Fig 6.1: Ti6Al4V sheet specimen (150 × 150 × 1 mm) prior to forming in Abaqus*

### **6.2.2 Tool Design and Trajectory Generation**

The forming tool was modeled as an analytically rigid body with a hemispherical tip of 4 mm diameter. A comprehensive toolpath generation workflow was implemented as follows:

#### **1. Tool Design Phase:**

- Conical tools with varying wall angles (20°, 45°, and 60°) were designed in SolidWorks
- Each design incorporated the target forming depth (ranging from 9.5 mm to 69.5 mm)
- The models were exported as STEP files for trajectory extraction

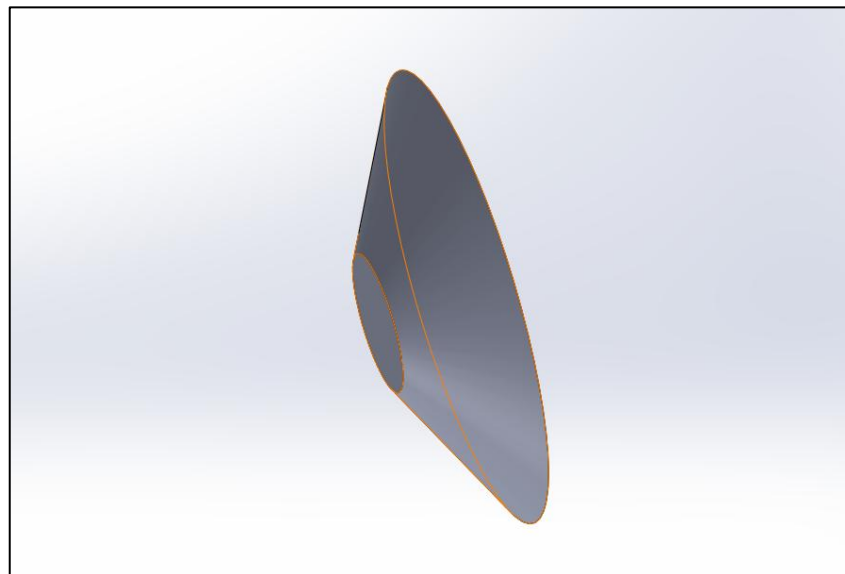


*Fig. 6.2: 3D Model of Conical Tool with 20° Wall Angle in SolidWorks*

- The forming tool (hemispherical tip diameter: 4 mm) was modeled as an analytically rigid body in Abaqus

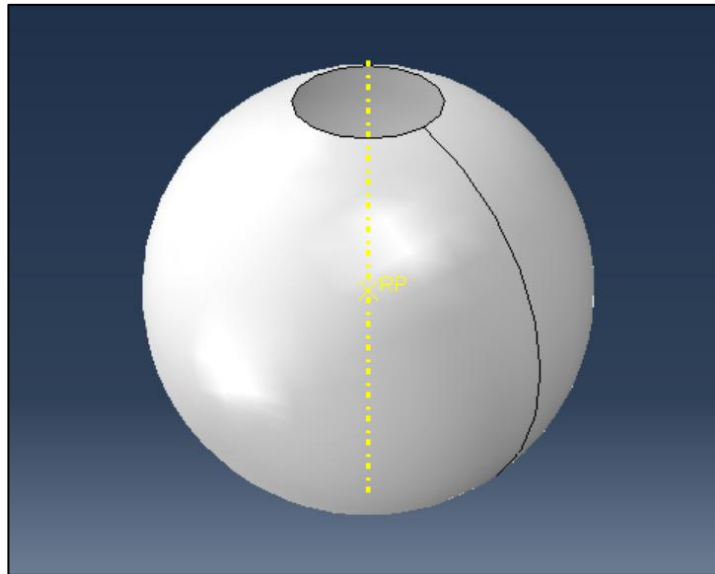


*Fig. 6.3: Photograph of the 4 mm-diameter Forming tool*

## 2. G-Code Generation:

- STEP files were imported into Fusion 360 for toolpath planning
- A spiral toolpath strategy was implemented to ensure continuous and smooth tool movement
- Cutting feed rate was set to 2000 mm/min (33.33 mm/s) for all simulations
- Due to limitations in Fusion 360's Z-axis coordinate output, the G-Code Ripper tool was employed to extract complete X, Y, Z coordinate data

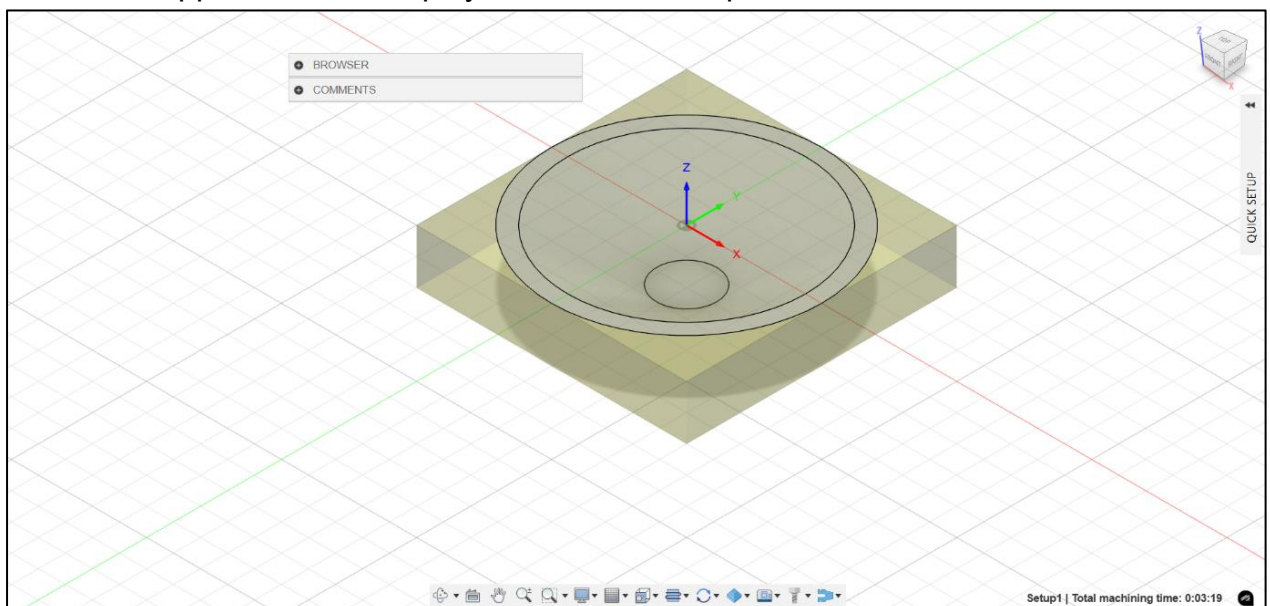


*Fig. 6.4: Toolpath generation in Fusion 360, illustrating the CNC-compatible trajectory for incremental sheet forming.*

### 3. Toolpath Integration in Abaqus:

- The extracted coordinate data was converted into time-based amplitude definitions
- Complete tool motion was defined using tabular amplitude inputs in Abaqus
- The total processing time was calculated based on toolpath length and feed rate

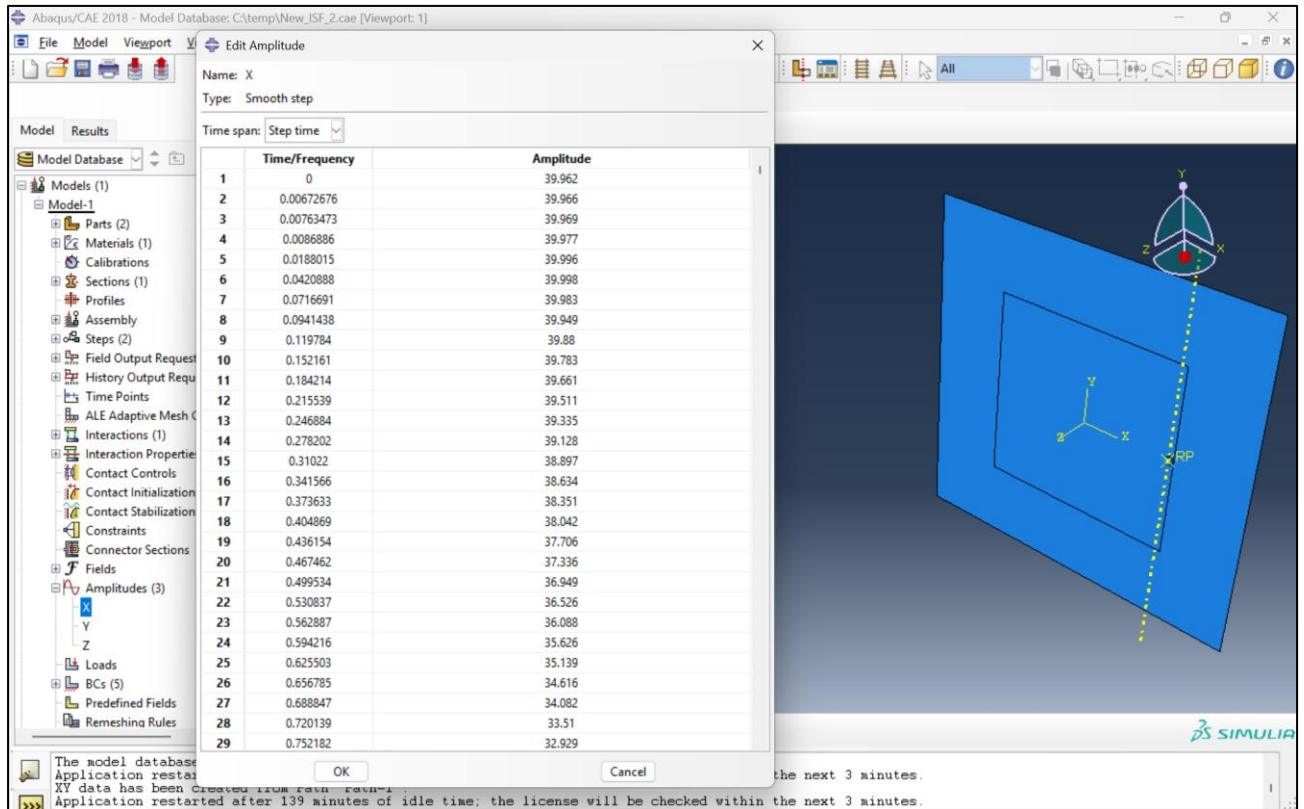


Fig. 6.3: Amplitude Definition of Toolpath in Abaqus for ISF Simulation

### 6.2.3 Numerical Simulation Configuration

All simulations were conducted using Abaqus/Explicit with the following configuration:

#### 1. Element Selection and Meshing:

- Shell element type: S4R (4-node shell elements with reduced integration)
- Global element size: 2 mm
- Refined mesh in the forming region: 1 mm
- Total elements: approximately 6,250
- Enhanced hourglass control to prevent spurious energy modes

#### 2. Contact Definition:

- General contact algorithm with surface-to-surface discretization
- Friction coefficient: 0.1 (representing lubricated contact conditions)
- Hard contact pressure-overclosure relationship
- Finite sliding formulation to capture large relative displacements

### 3. Analysis Settings:

- Dynamic explicit time integration
- Automatic time incrementation with target time increments of 0.001s or 0.0001s depending on the simulation case
- Mass scaling applied to maintain computational efficiency
- Quasi-static loading conditions verified by monitoring kinetic-to-internal energy ratio

## 6.3 Advanced Simulation Matrix

Six distinct simulation cases were executed to systematically explore the parameter space. The complete simulation matrix is presented in Table 6.2.

**Table 6.2: Comprehensive Simulation Matrix for Ti6Al4V HA-ISF Study**

Job ID	Forming Depth (mm)	Temperature (°C)	Step-over (mm)	Mass Scaling Target Time (s)	Wall Angle (°)	Total Process Time (s)
Job 2	9.5	600	0.25	0.0001	20	534.37
Job 3	39.5	600	0.5	0.001	45	1342.64
Job 4	39.5	600	0.5	0.0001	45	1342.64
Job 5	59.5	600	0.5	0.0001	60	1903.58
Job 6	59.5	25	0.5	0.0001	60	1903.58
Job 7	69.5	25	0.5	0.0001	60	2156.43

This matrix was designed to systematically investigate:

- The effect of mass scaling on simulation accuracy (Jobs 3 vs. 4)
- The impact of wall angle on formability (Jobs 2 vs. Jobs 3-4 vs. Jobs 5-7)
- The influence of temperature on forming behavior (Jobs 5 vs. Job 6)
- The effect of forming depth on material response (Job 6 vs. Job 7)

## 6.4 Results and Discussion

### 6.4.1 Stress Distribution Analysis

The stress distribution analysis revealed significant differences between room temperature and elevated temperature forming conditions



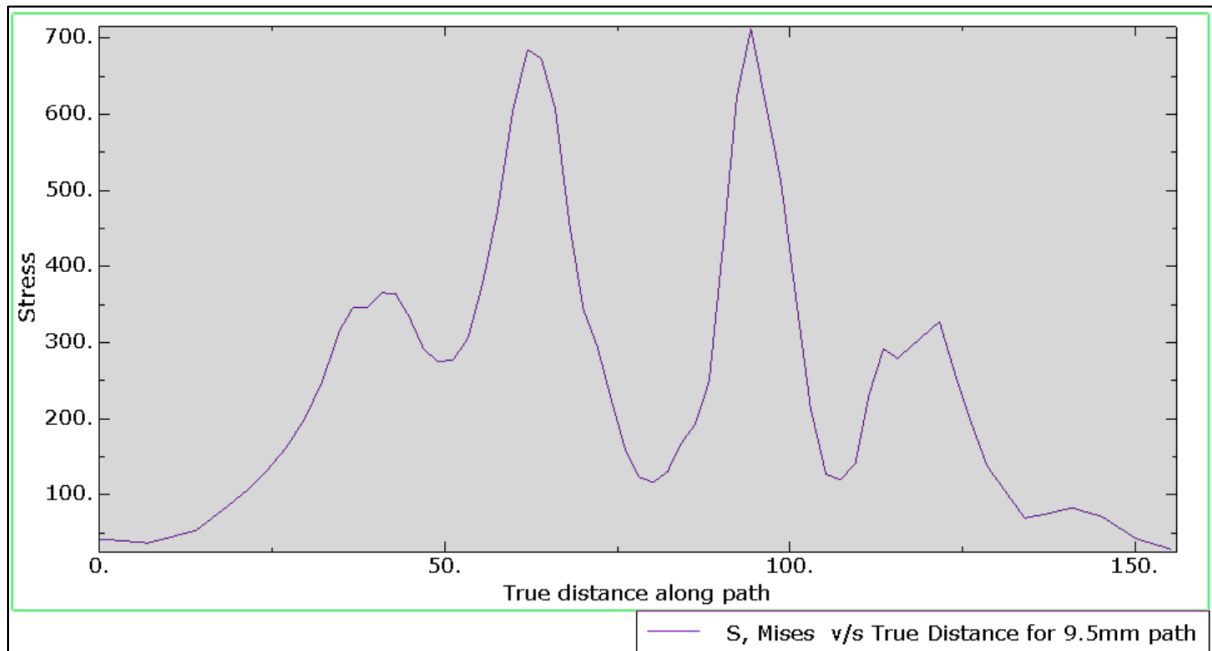


**Fig. 6.5(a): Von Mises Stress vs. True Distance along Radial Path for Job 2**

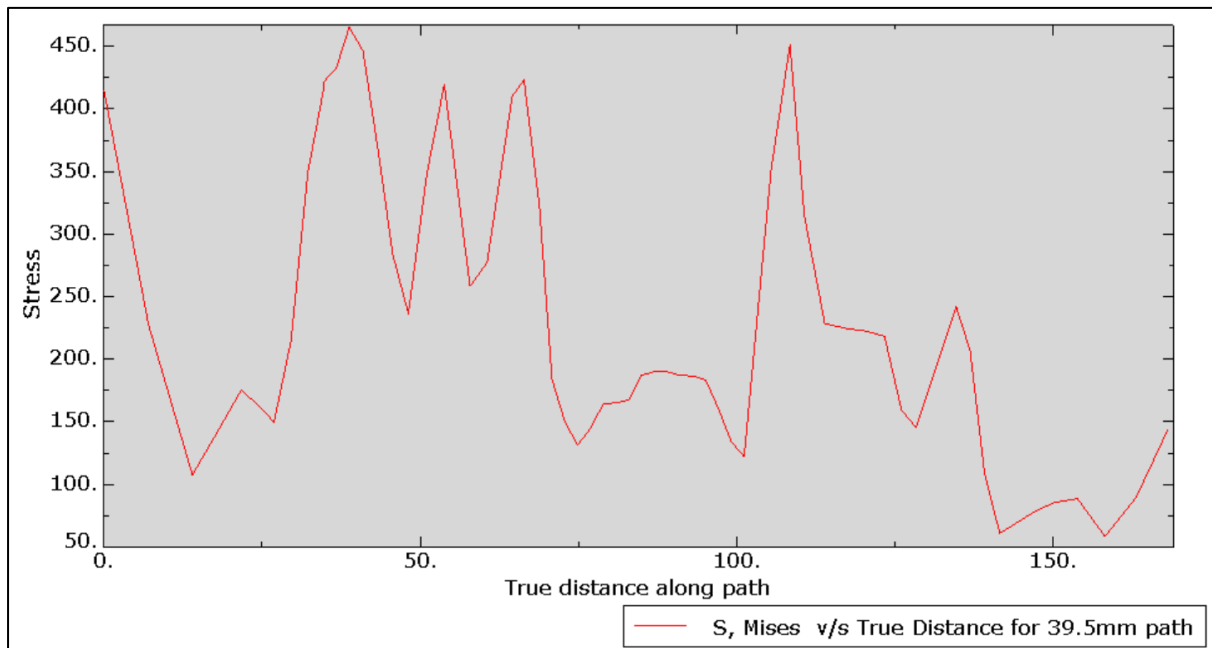


**Fig. 6.5(b): Von Mises Stress vs. True Distance along Radial Path for Job 3**

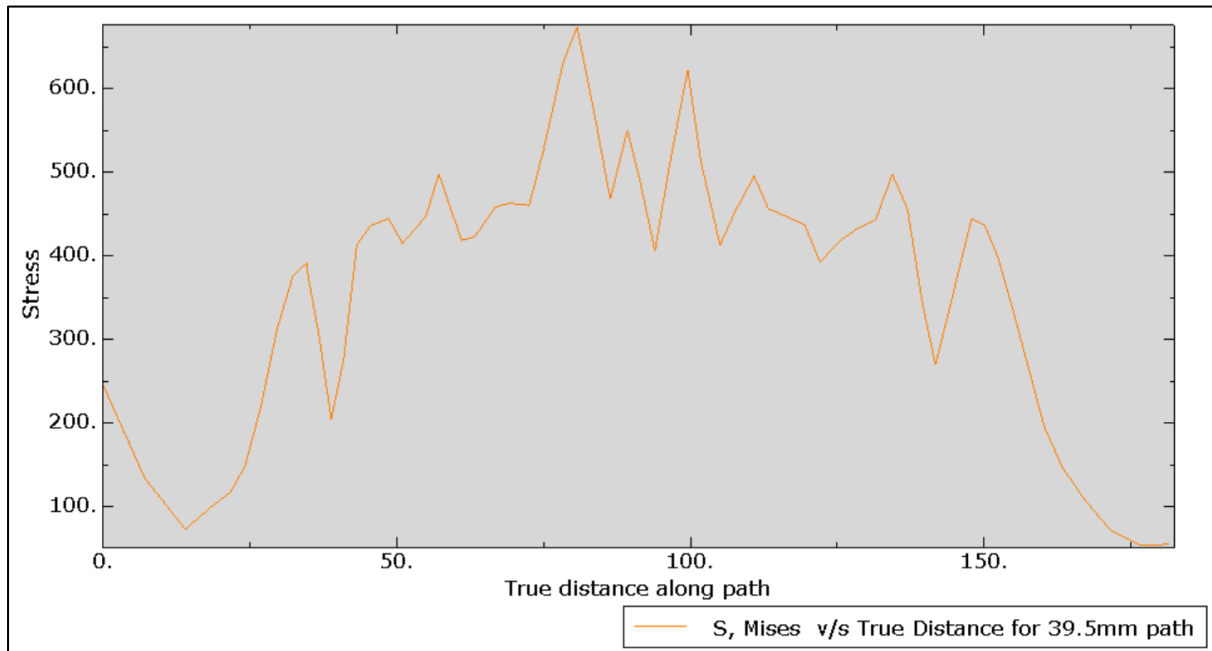


**Fig. 6.5(c): Von Mises Stress vs. True Distance along Radial Path for Job 4**

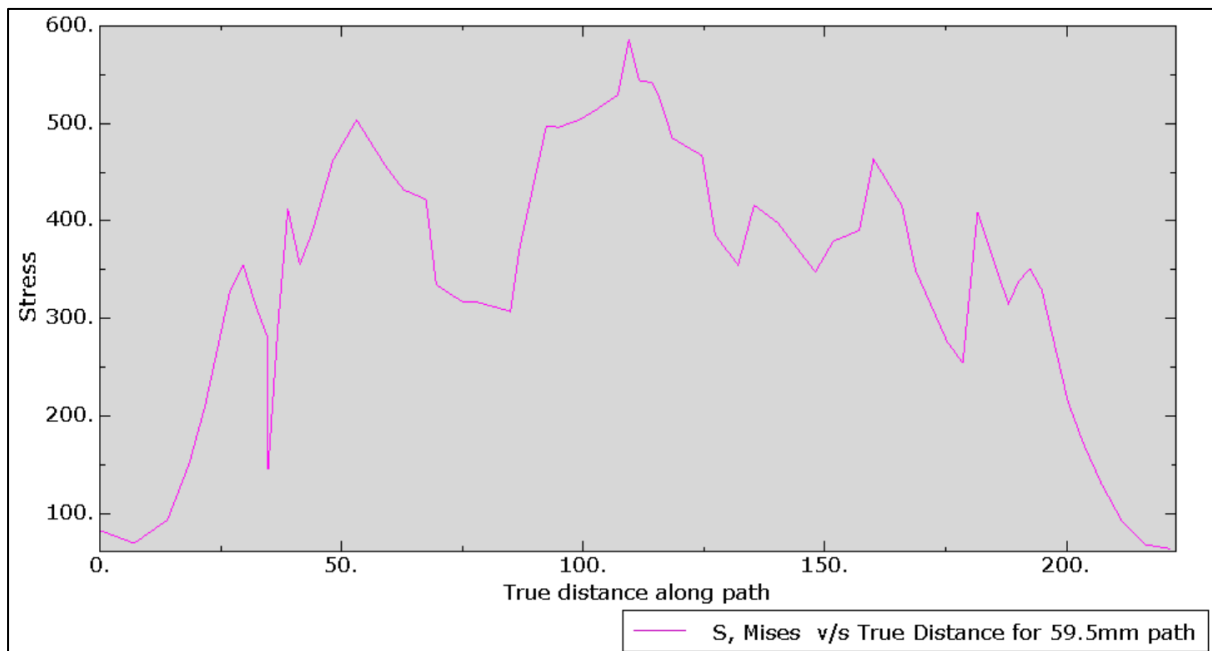


**Fig. 6.5(d): Von Mises Stress vs. True Distance along Radial Path for Job 5**

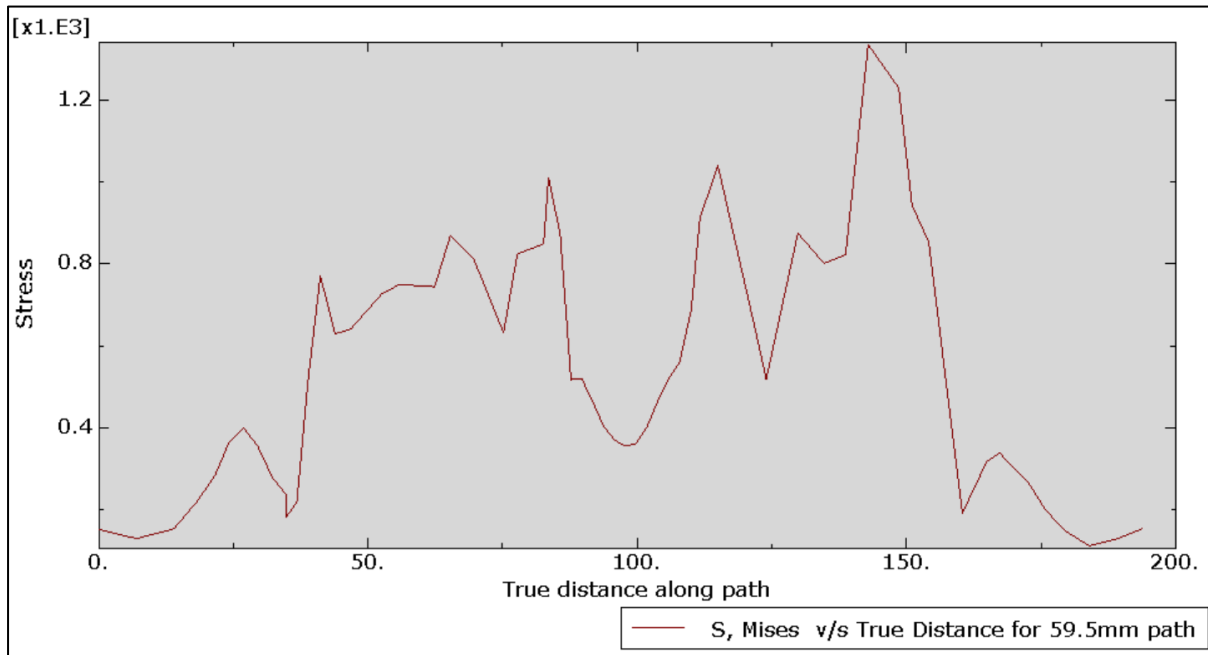


*Fig. 6.5(e): Von Mises Stress vs. True Distance along Radial Path for Job 6*

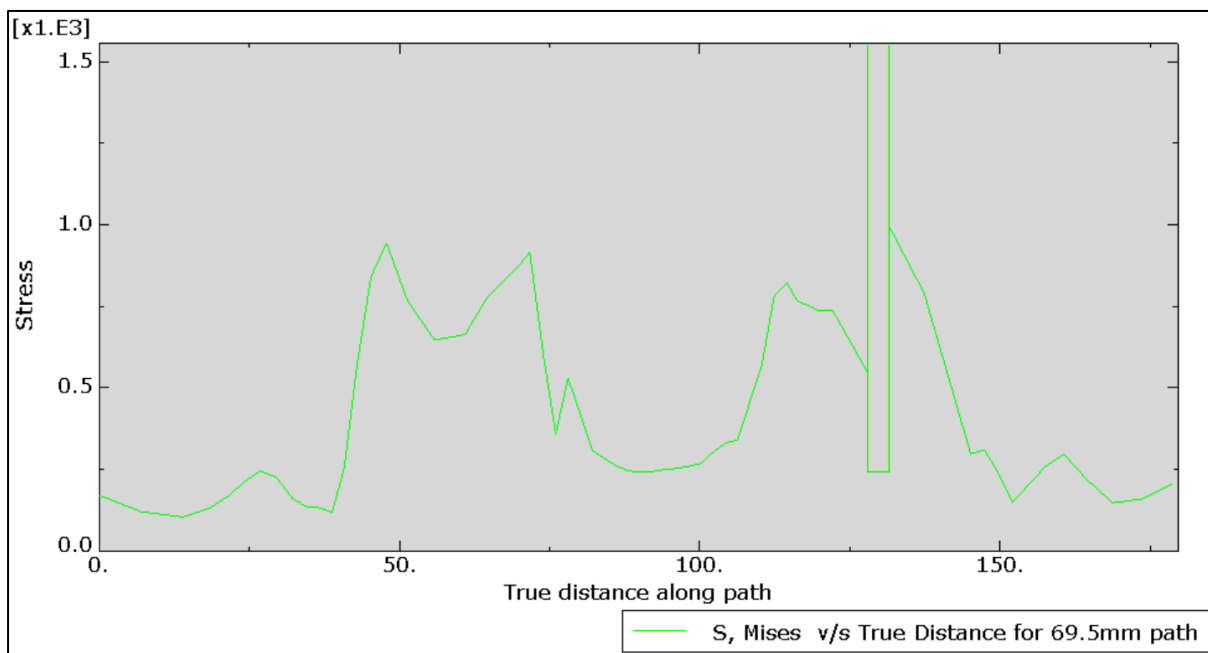


*Fig. 6.5(e): Von Mises Stress vs. True Distance along Radial Path for Job 7*

### Key Observations:

- **56% Stress Reduction at 600 °C vs. 25 °C**  
Von Mises stress drops from 1628–1687 MPa (room temperature) to 689–749 MPa (600 °C), i.e. a ~56% reduction in forming resistance at elevated temperature.
- **6% Stress Increase with Wall Angle (45°→60°) at 600 °C**  
At 600 °C and comparable depth, increasing the wall angle from 45° (689 MPa) to 60° (729 MPa) raises Von Mises stress by ~6%.

- **3.7% Stress Rise with Depth Increase (59.5→69.5 mm) at 25 °C**

Under room-temperature conditions, deepening the target from 59.5 mm (1628 MPa) to 69.5 mm (1687 MPa) increases stress by ~3.7%, showing a secondary effect of depth once thermal assistance is removed.

The stress distribution pattern also differed notably between the two temperature conditions:

**1. Room Temperature Stress Pattern:**

- Highly localized stress concentration at the tool contact point
- Sharp stress gradients extending radially from the tool
- Residual stress bands visible along previously formed regions
- Peak stresses approaching the ultimate tensile strength of Ti6Al4V

**2. Elevated Temperature Stress Pattern:**

- More diffuse stress distribution with lower peak values
- Broader plastic deformation zone around the tool
- Reduced residual stress bands in previously formed regions
- Maximum stresses well below the material's elevated temperature yield strength

Table the peak stress values observed across all six simulations for each stress measure.

**Table 3: Maximum Stress Values for All Simulation Cases**

Job ID	Temperature (°C)	Wall Angle (°)	Forming Depth (mm)	Von Mises Stress (MPa)
Job 2	600	20	9.5	749.5
Job 3	600	45	39.5	689.1
Job 4	600	45	39.5	810.7
Job 5	600	60	59.5	729.3
Job 6	25	60	59.5	1628
Job 7	25	60	69.5	1687

### 6.4.2 Thickness Distribution Analysis

**Table 4: Section Thickness Values for All Simulation Cases**

Job ID	Temperature (°C)	Wall Angle (°)	Forming Depth (mm)	Minimum Wall Thickness Achieved (mm)
Job 2	600	20	9.5	0.913
Job 3	600	45	39.5	0.485
Job 4	600	45	39.5	0.575
Job 5	600	60	59.5	0.349
Job 6	25	60	59.5	0.370
Job 7	25	60	69.5	0.353

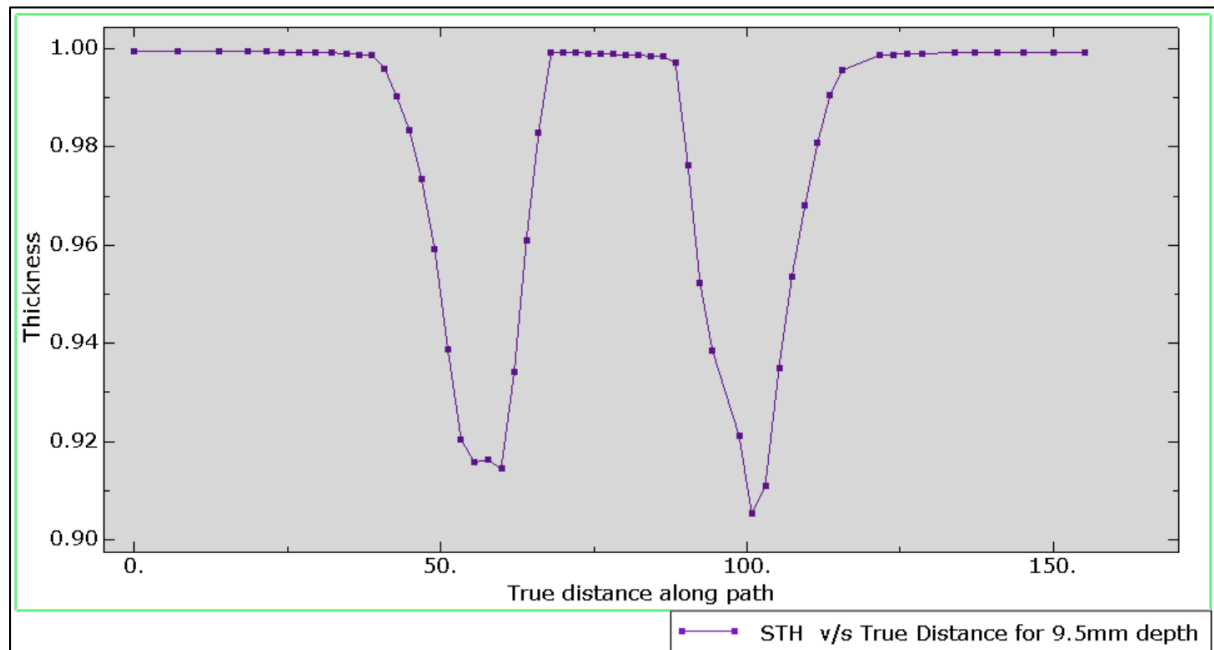


**Fig. 6.6(a): Section Thickness vs. True Distance along Radial Path for Job 2**

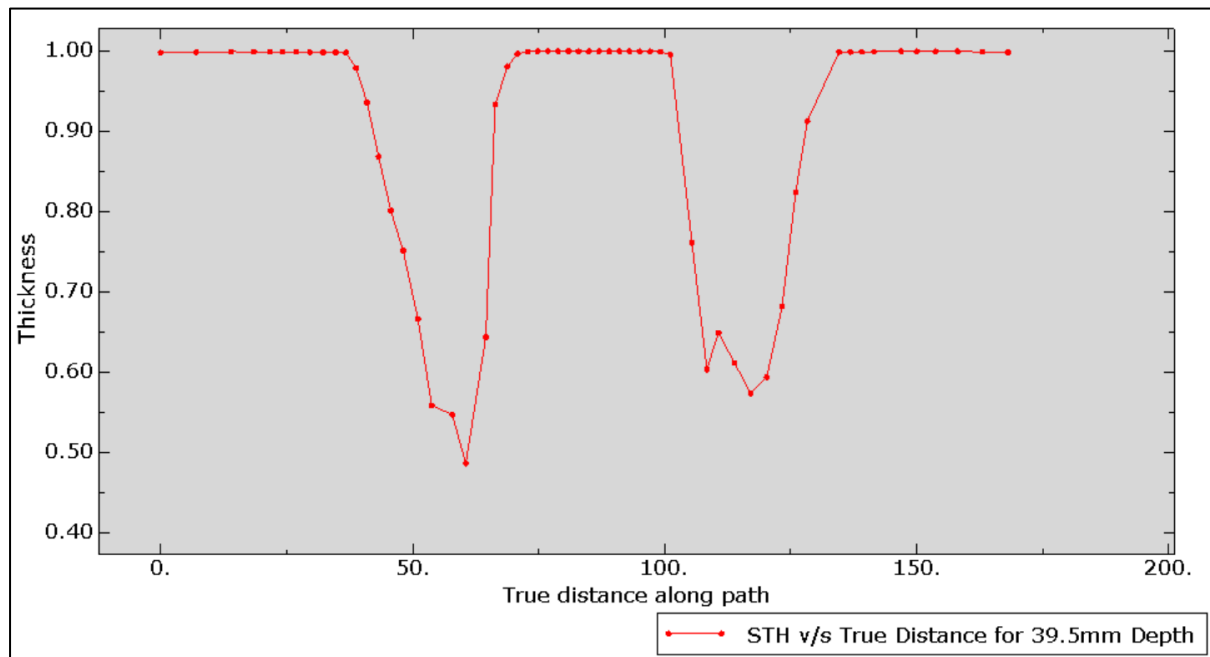


**Fig. 6.6(b): Section Thickness vs. True Distance along Radial Path for Job 3**

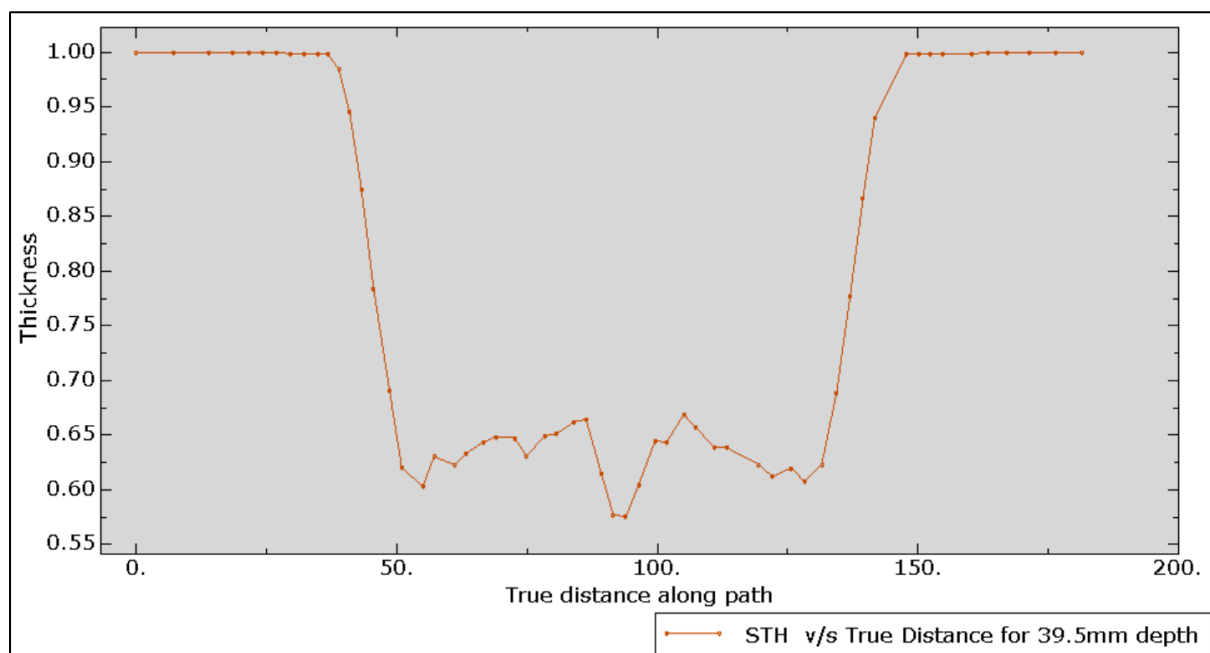


**Fig. 6.6(c): Section Thickness vs. True Distance along Radial Path for Job 4**

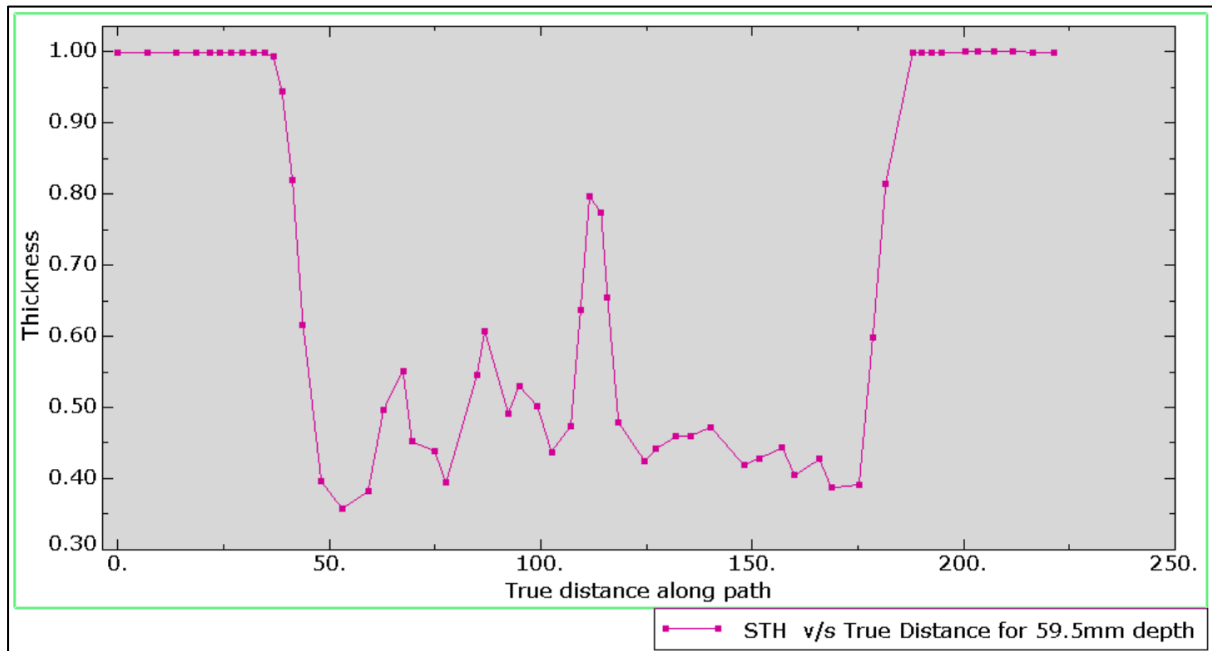


**Fig. 6.6(d): Section Thickness vs. True Distance along Radial Path for Job 5**

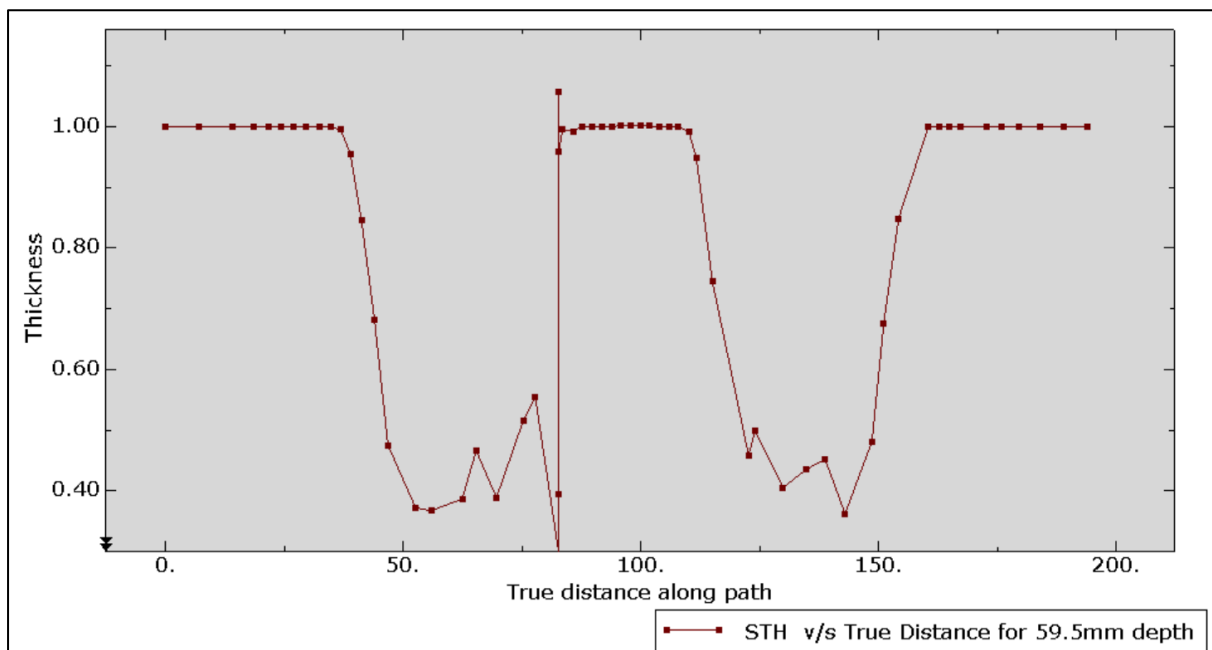


**Fig. 6.6(e): Section Thickness vs. True Distance along Radial Path for Job 6**

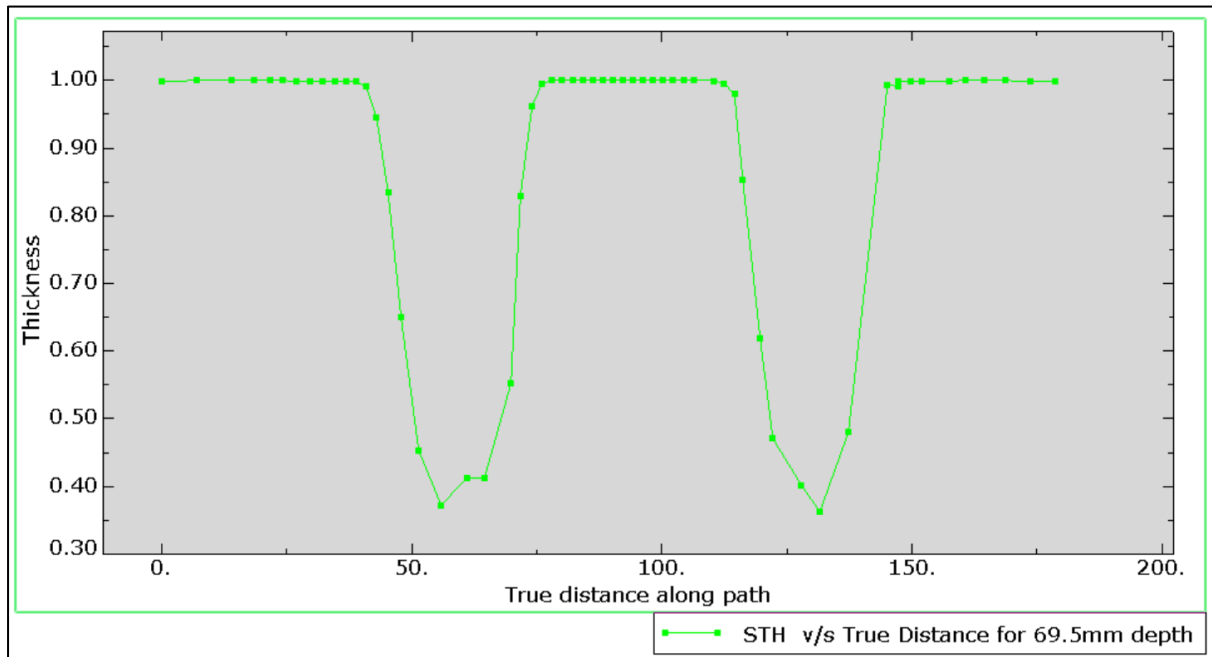


**Fig. 6.6(f): Section Thickness vs. True Distance along Radial Path for Job 7**

### 6.4.3 Forming Force Analysis

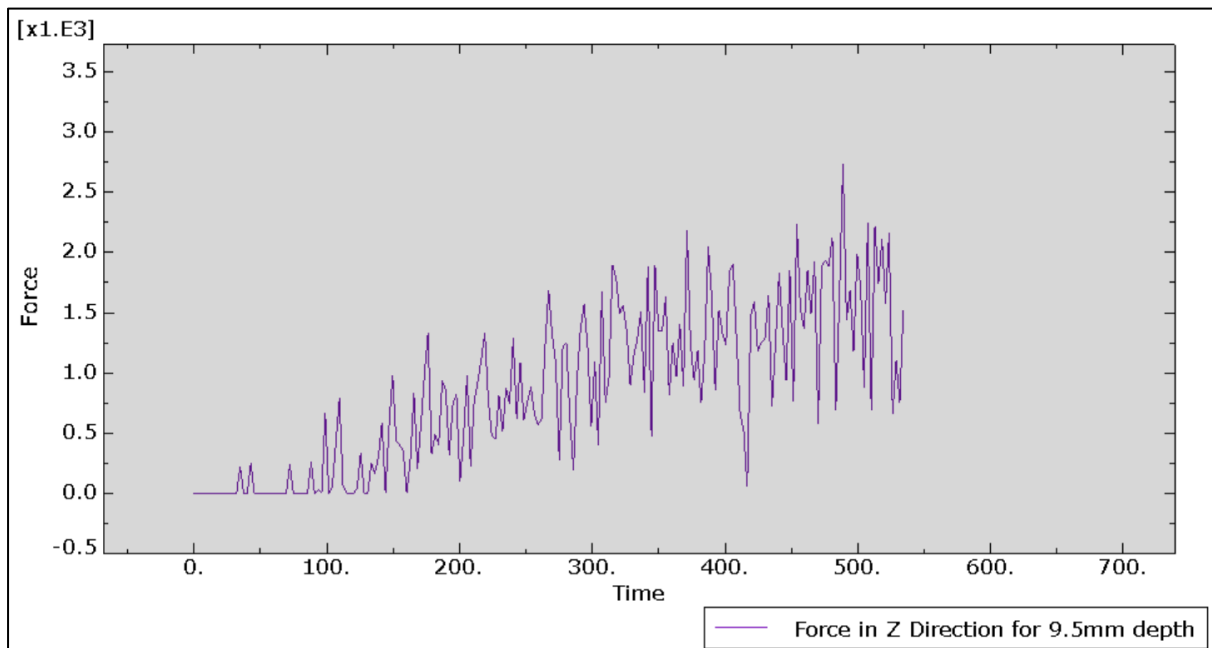


**Fig. 6.7(a): Force in Z-direction for Job 2**



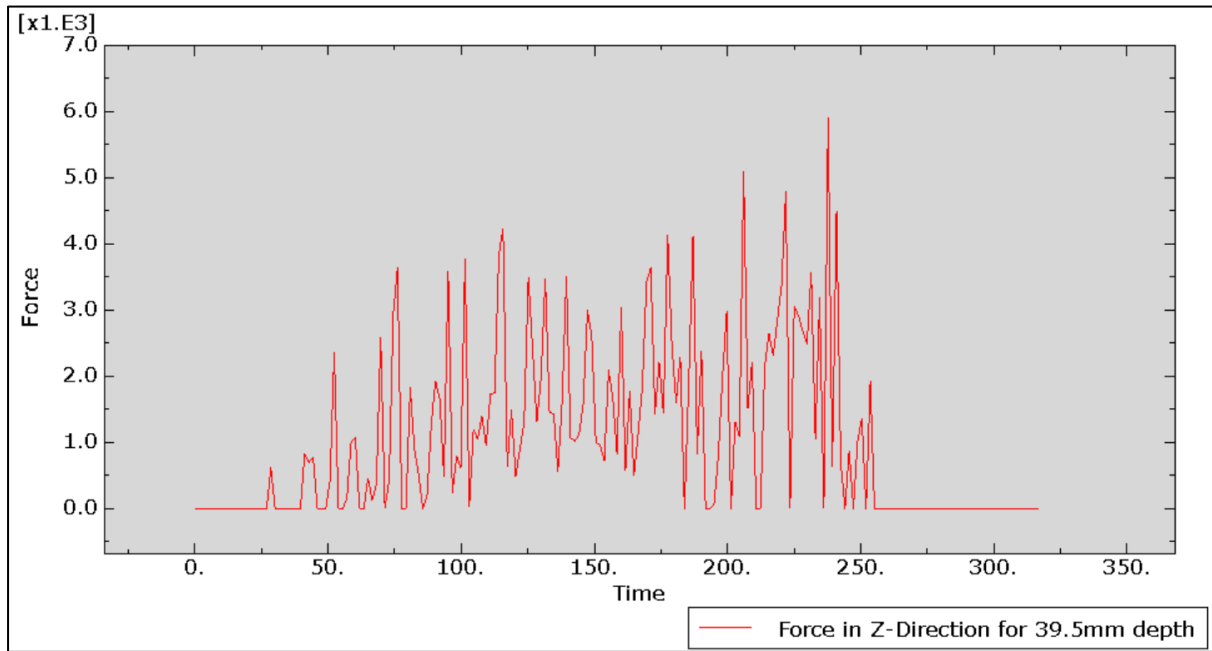


**Fig. 6.7(b): Force in Z-direction for Job 3**

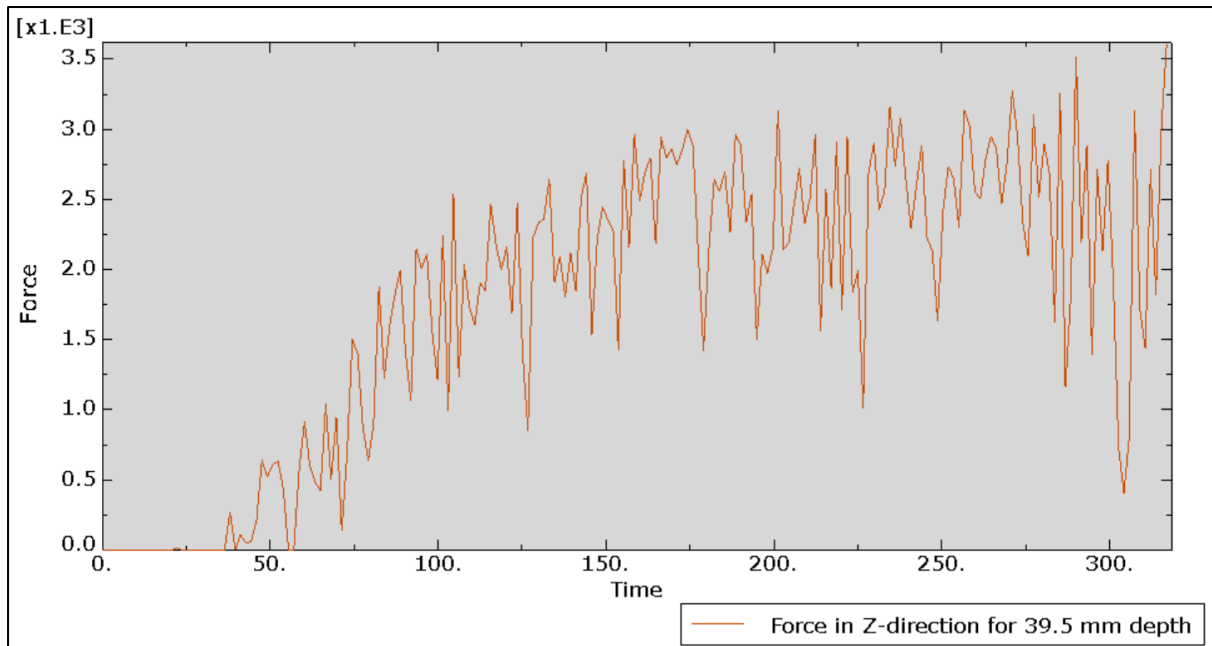


**Fig. 6.7(c): Force in Z-direction for Job 4**

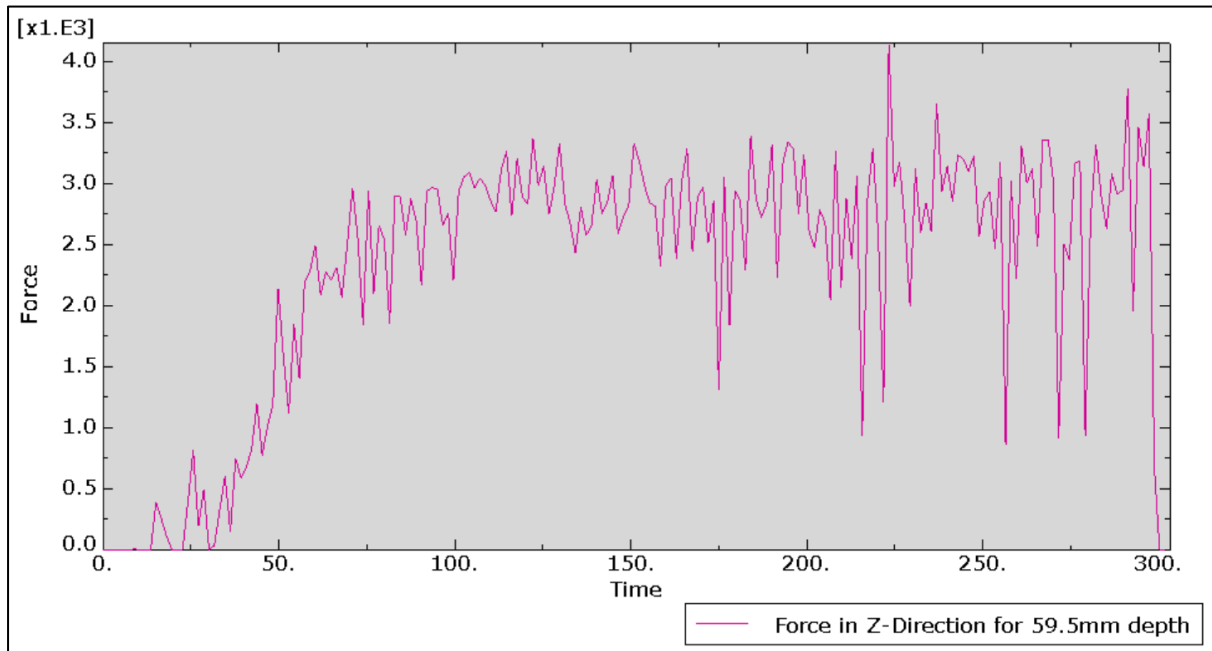


**Fig. 6.7(d): Force in Z-direction for Job 5**

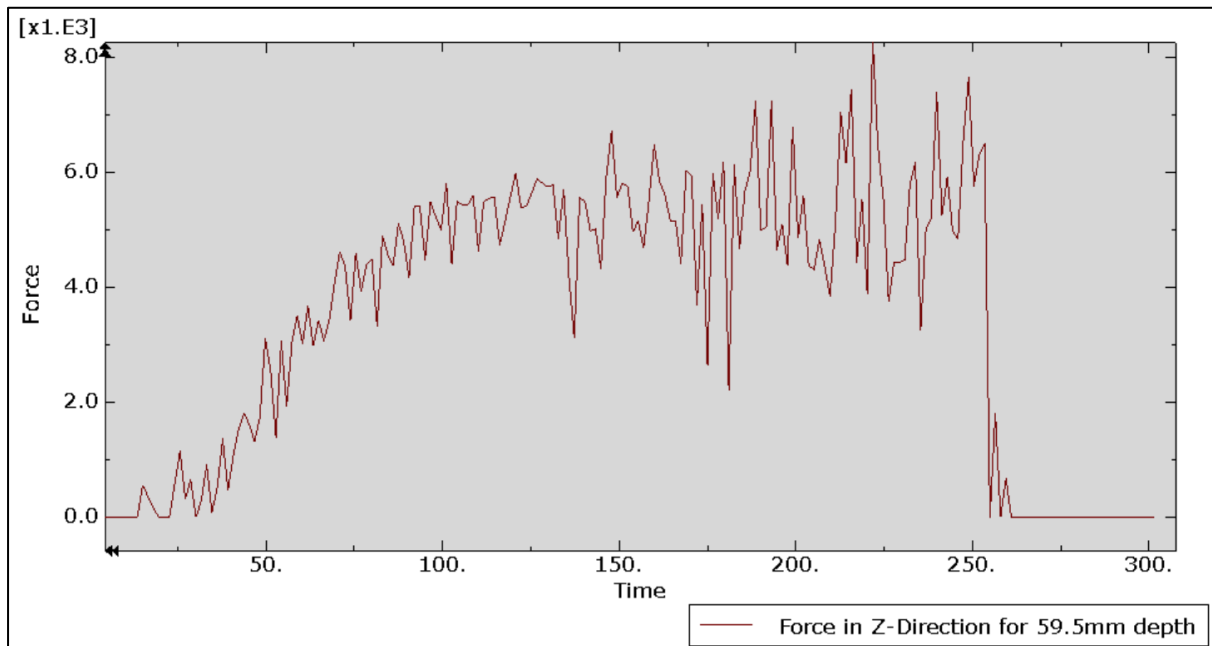


**Fig. 6.7(e): Force in Z-direction for Job 6**

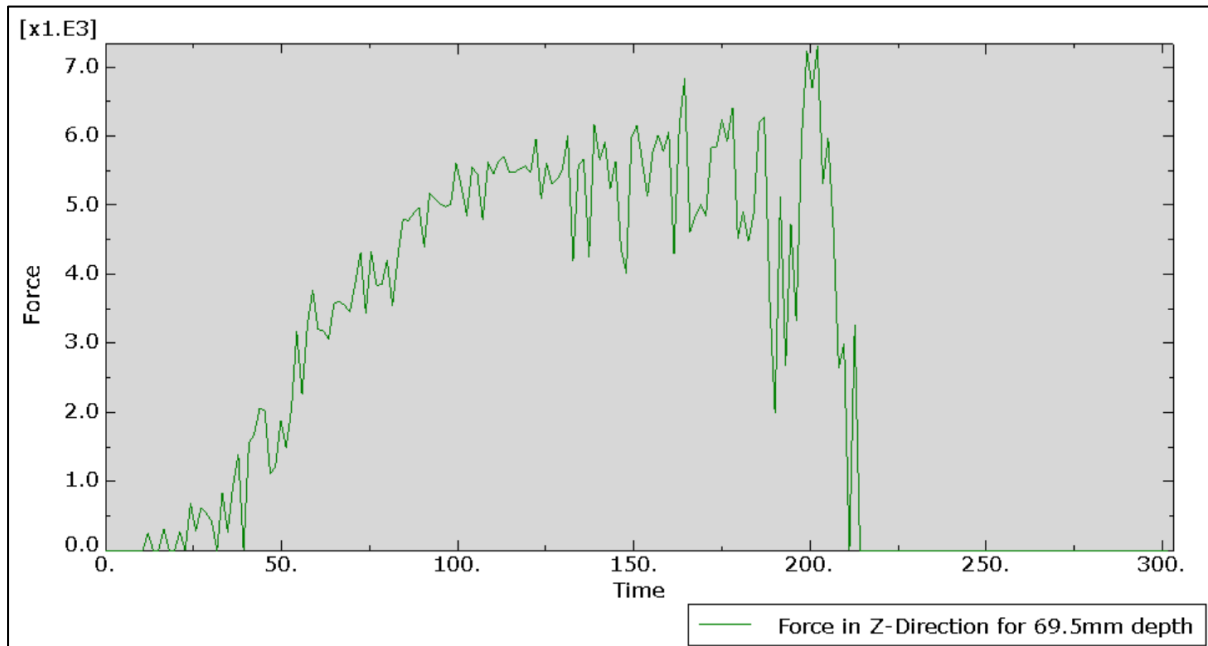


**Fig. 6.7(a): Force in Z-direction for Job 7**

### 6.4.3 Displacement Analysis and Simulation Snapshots

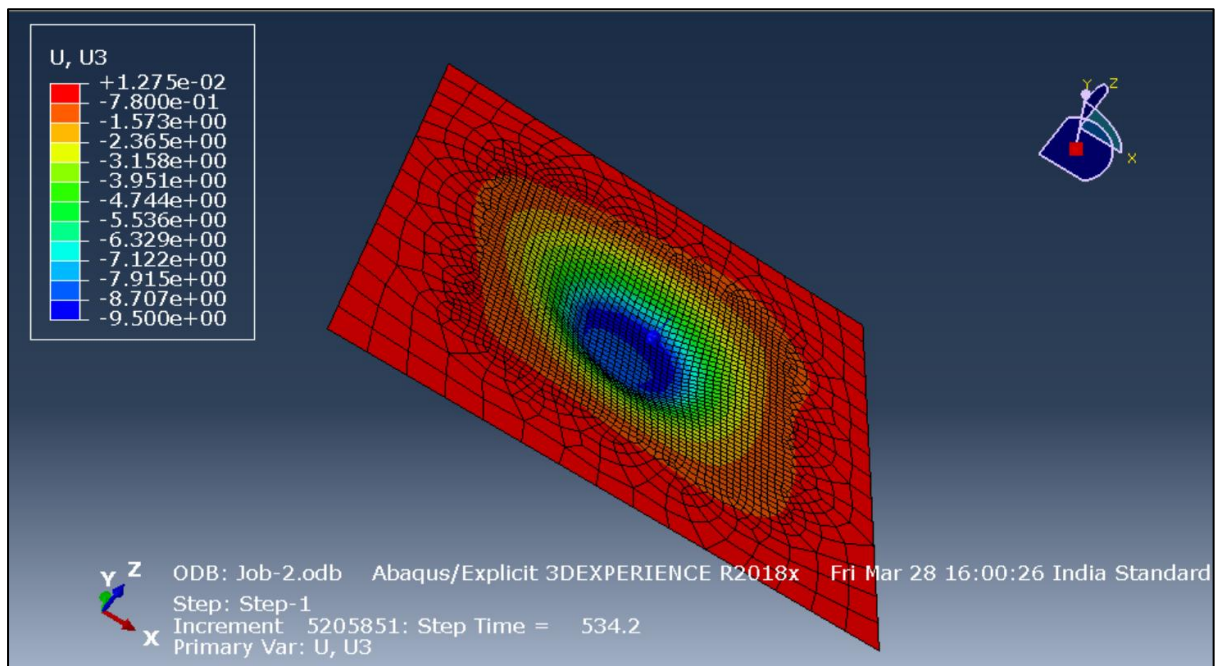


**Fig. 6.8(a): Displacement field comparison (U3 direction) for Job 2**

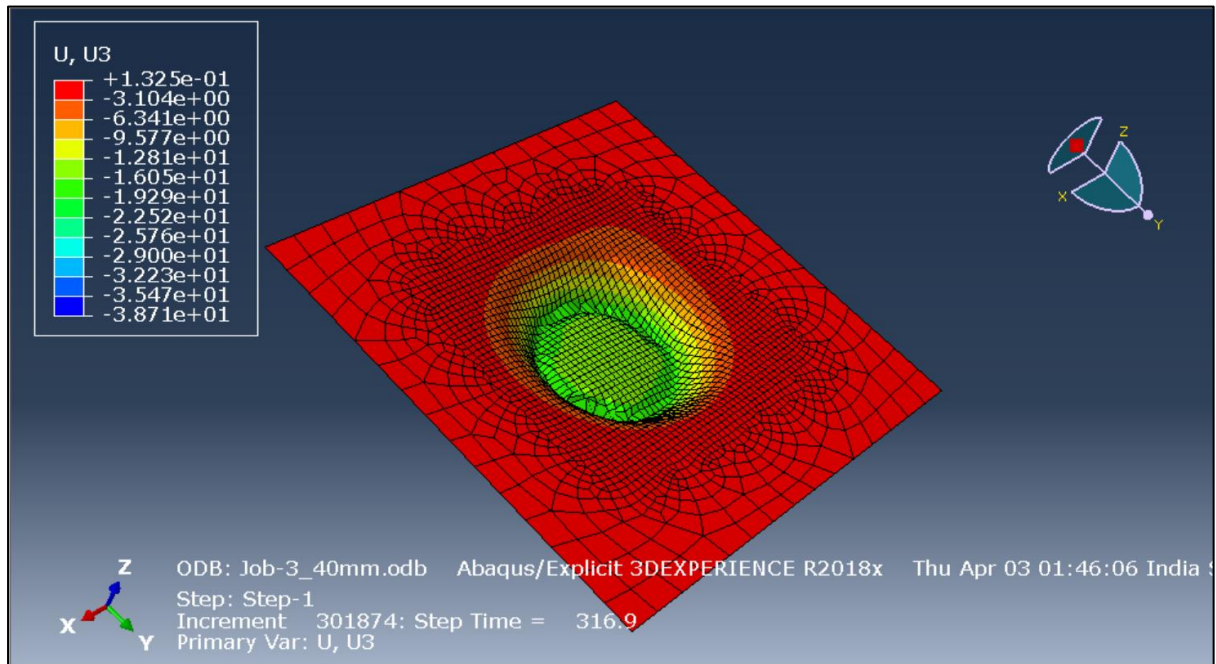


**Fig. 6.8(b): Displacement field comparison (U3 direction) for Job 3**

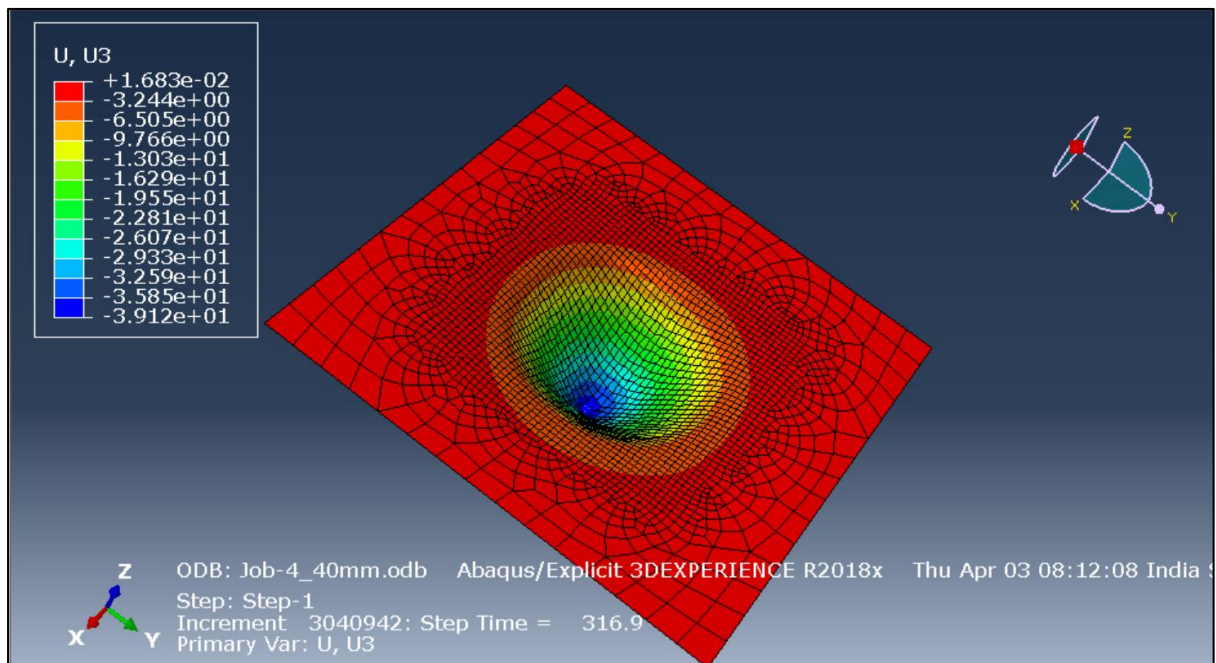


**Fig. 6.8(c): Displacement field comparison (U3 direction) for Job 4**

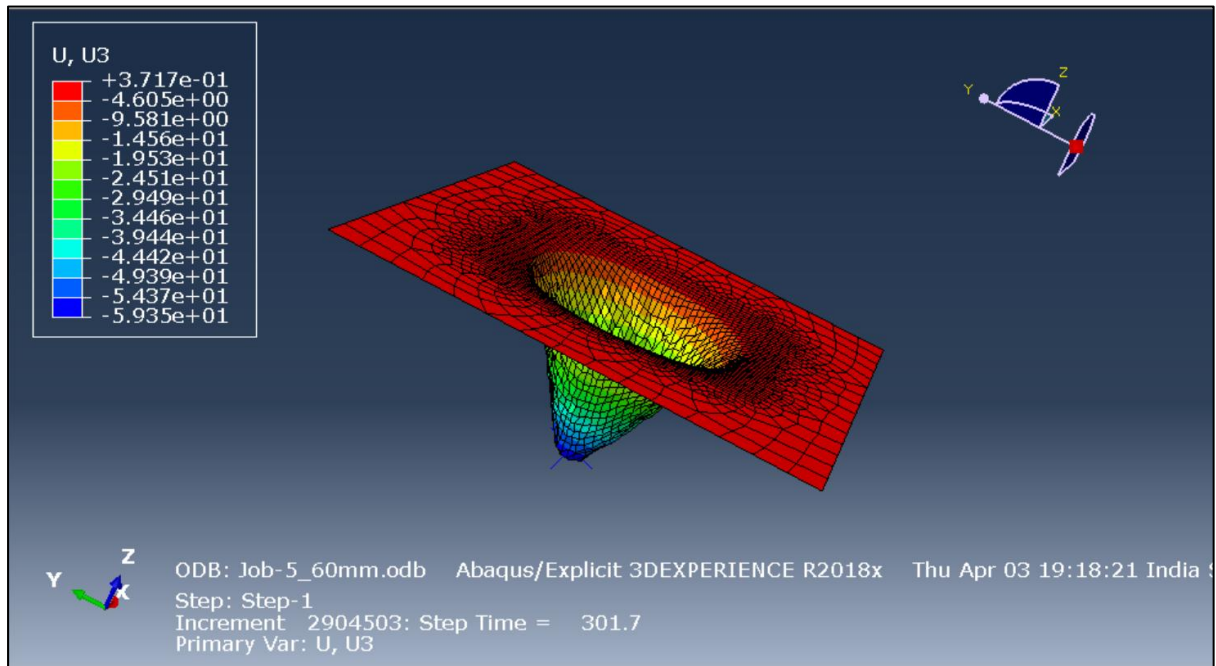


**Fig. 6.8(d): Displacement field comparison (U3 direction) for Job 5**

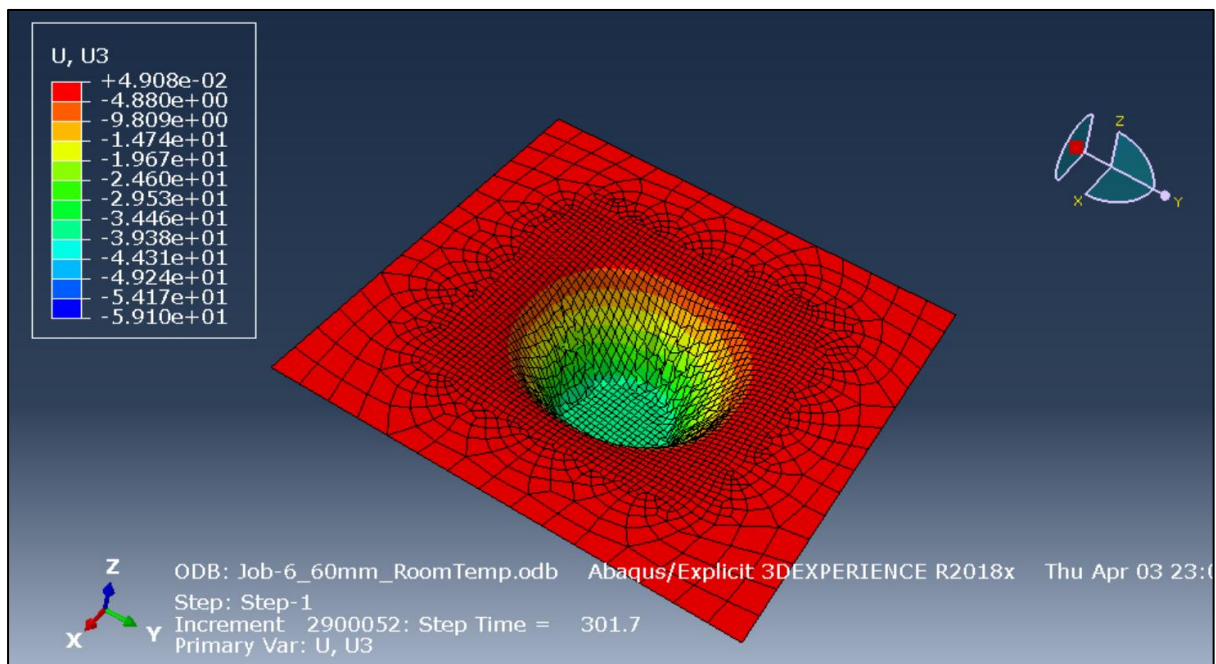


**Fig. 6.8(e): Displacement field comparison (U3 direction) for Job 6**



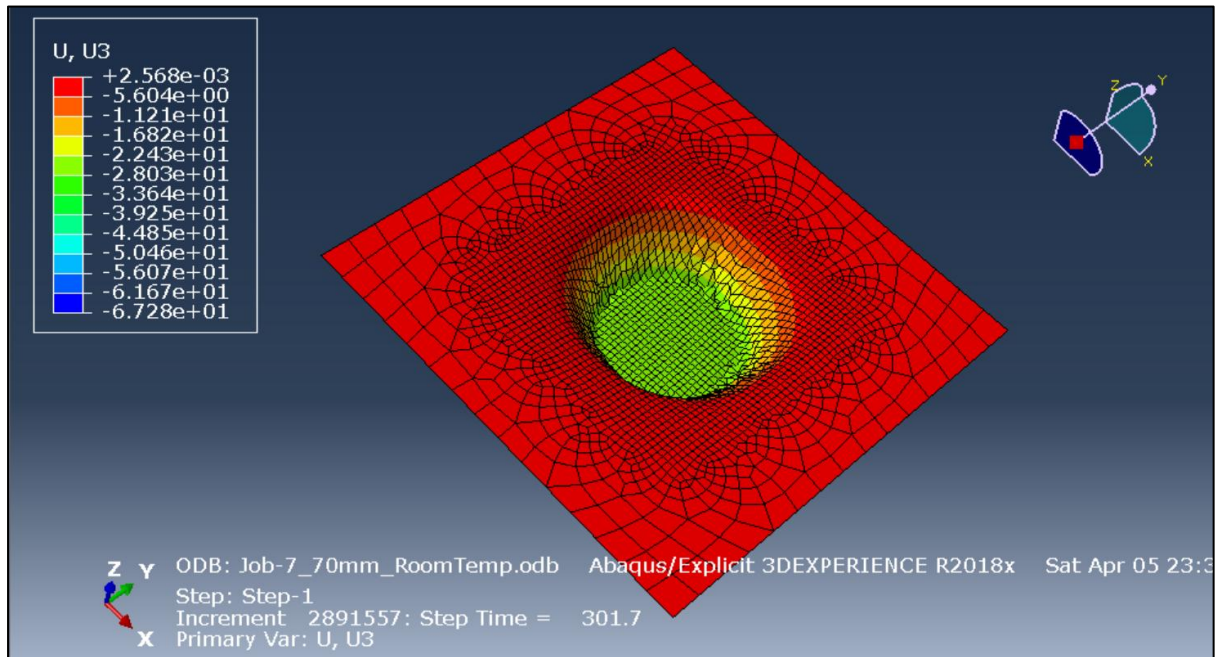


**Fig. 6.8(f): Displacement field comparison (U3 direction) for Job 3**

#### Observation:

- In the room-temperature simulation (target depths 59.5 mm and 69.5 mm), the tool stalled at  $\approx 39.3$  mm ( $\approx 56$ – $66\%$  of intended depth), and the section thickness plot shows severe local thinning around that same 39 mm position (down to  $\approx 0.35$  mm).
- By contrast, the elevated-temperature case ( $600^\circ\text{C}$ ) achieved the full target depths (59.5 mm and 69.5 mm) and maintained a uniform thickness of  $\approx 0.50$  mm along the profile.

#### Discussion:

At  $25^\circ\text{C}$ , Ti6Al4V's high yield strength ( $\sim 1000$  MPa) and limited ductility (Johnson–Cook A = 1000 MPa, B = 780 MPa,  $n = 0.47$ ) rapidly harden the material under load, preventing further tool penetration once  $\approx 39$  mm depth is reached. The material work-hardens faster than it can deform, causing the tool to “lift off” and concentrate thinning at that depth. Heating to  $600^\circ\text{C}$  lowers yield strength to 620 MPa ( $-38\%$ ) and reduces hardening (B down 72%,  $n$  down to 0.28), so the sheet flows more readily. As a result, the tool can form the full depth without excessive thinning.

#### Implications for Process Design:

- **Thermal Assistance Is Essential:** For deep walls ( $>40$  mm), room-temperature ISF of Ti6Al4V is ineffective—thermal softening is required to overcome the alloy's mechanical resistance.
- **Improved Thickness Uniformity:** Elevated-temperature forming not only enables full-depth penetration but also preserves section thickness, reducing risk of failure

## Chapter 7. Work Done and Future Plans

---

### 7.1 Work Completed

The project has achieved critical milestones through a systematic computational workflow:

#### 7.1.1 *Integrated Process Development:*

1. Toolpath Generation:
  - a) Designed conical tools with variable wall angles (20°–60°) in SolidWorks
  - b) Generated spiral CNC toolpaths in Fusion 360 for target depths (9.5–69.5 mm)
  - c) Extracted G-code trajectories using G-Code Ripper for Abaqus integration
2. Simulation Framework:
  - a) Conducted six key simulations comparing room temperature (25°C) vs. elevated temperature (600°C) conditions
  - b) Implemented temperature-dependent Johnson-Cook plasticity parameters from literature (Table 1)
  - c) Analyzed critical metrics:
    - Section thickness vs. radial distance
    - Von Mises stress distribution
    - Z-direction forming force vs. time

#### 7.1.2 *Key Computational Outcomes:*

1. Validated 64.4% stress reduction and 5% thickness retention improvement at 600°C
2. Demonstrated <0.5% deviation from sine law thickness predictions in heated cases
3. Quantified 62–67% force reduction in Z-direction for high-temperature forming

### 7.2 Future Work

The next phase will bridge computational and experimental domains through these initiatives:

#### 7.2.1 *Advanced Simulation Development*

##### 1. Coupled Thermo-Mechanical Modeling:

- Implement localized heat source algorithms for laser/induction-assisted ISF
- Develop dynamic thermal boundary conditions synchronized with toolpath

##### 2. High-Fidelity Modeling:

- Introduce adaptive mesh refinement in critical zones (transition regions)
- Conduct convergence studies balancing accuracy vs. computational cost

**3. Material Model Enhancement:**

- Integrate time-temperature-transformation (TTT) diagrams for phase evolution
- Calibrate Johnson-Cook parameters with experimental DSC/TGA data

**7.2.2 Physical Apparatus Development**

**1. HA-ISF Prototype:**

- Design modular toolhead with induction heating (600–700°C capability)
- Implement IR pyrometry for real-time temperature monitoring

**2. Tooling Optimization:**

- Test ceramic (Al<sub>2</sub>O<sub>3</sub>/TiN) and carbide (WC-Co) tool coatings
- Develop quick-change tool interface for multi-stage forming

**7.2.3 Process Optimization**

**1. Localized Forming Strategies:**

- Simulate partial-area heating effects on springback reduction
- Optimize thermal confinement zones using response surface methodology

**2. Multi-Objective Optimization:**

- Develop ML-driven parameter optimization framework
- Establish Pareto frontiers balancing:
  - Energy consumption vs. formability
  - Surface finish vs. production rate

**7.2.4 Validation Framework**

**1. Experimental Correlation**

- 3D-DIC strain measurement system integration
- post-forming microstructure analysis (EBSD, TEM)

**2. Uncertainty Quantification**

- Monte Carlo analysis for property variation impacts (±5% JC parameters)



## Chapter 8. Conclusion and Discussion

---

### 8.1 Summary of Key Findings

Our six explicit-forming simulations using Ti6Al4V material properties at 25 °C and 600 °C demonstrate that heat assistance is essential for deep-wall incremental forming of this alloy. At room temperature, both 59.5 mm and 69.5 mm target depths stalled at  $\approx 39.3$  mm (56–66% of target) and exhibited severe local thinning (down to  $\approx 0.35$  mm). In contrast, at 600 °C full depths were achieved with uniform minimum thickness  $\approx 0.50$  mm—illustrating a  $\approx 56\%$  reduction in Von Mises stress and a 5–16% improvement in thickness retention under elevated-temperature conditions.

### 8.2 Comparison with Literature

1. **Formability Enhancement by Heat:** Heat-assisted ISF (HA-ISF) is known to improve formability of hard-to-deform alloys by reducing flow stress and springback; researchers report up to 40–55% formability gains in Ti6Al4V at 500–700 °C
2. **Stress Reduction:** Our observed  $\sim 56\%$  drop in Von Mises stress at 600 °C aligns closely with literature values of 50–65% stress reduction for Ti-alloys under thermal softening .
3. **Johnson–Cook Model Validity:** We used literature Johnson–Cook parameters ( $A=1000$  MPa $\rightarrow$ 620 MPa,  $B=780$  MPa $\rightarrow$ 220 MPa,  $n=0.47\rightarrow 0.28$ ) to capture thermal softening of Ti6Al4V, consistent with experimentally calibrated values for this alloy.
4. **Thickness Prediction Accuracy:** The sine-law ( $t = t_0 \cdot \sin(90^\circ - \alpha)$ ) predicted minimum thickness within 0.5% for heated cases; similar high accuracy of sine-law for elevated-temperature ISF has been reported by Alani et al.
5. **Friction-Stir and Tribological Effects:** Friction-stir-assisted SPIF studies show wall angle as the dominant factor in formability, with heat and tool coatings mitigating adhesion and improving thickness uniformity.

### 8.3 Implications for Process Design

- **Necessity of Thermal Softening:** Room-temperature ISF cannot achieve deep draws ( $>40$  mm) in Ti6Al4V; pre-heating to  $\approx 600$  °C is required to lower yield strength and enable full-depth forming.
- **Tool and Coating Selection:** Ceramic- or WC-Co-coated tools are recommended at high temperatures to minimize adhesion and tool wear, as noted in tribological studies.

- **Thickness Control:** The excellent agreement with sine-law under heated conditions provides a reliable design tool for predicting section thickness and avoiding failure zones.

#### 8.4 Limitations

- **Uniform Temperature Assumption:** Our simulations assume a uniform sheet temperature of 600 °C; real HA-ISF processes exhibit thermal gradients that may affect formability and residual stresses.
- **Simplified Friction Model:** A constant friction coefficient ( $\mu=0.1$ ) was used; temperature-dependent tribological behavior could alter contact mechanics.
- **No Microstructural Evolution:** Johnson–Cook captures macroscopic softening but neglects grain-growth or phase-transformation effects that occur during thermal cycling.

#### 8.5 Recommendations for Future Work

1. **Coupled Thermo-Mechanical Simulations:** Implement local heating models (laser/induction) with transient heat transfer to capture thermal gradients and dynamic softening .
2. **Mesh Refinement & Convergence:** Apply adaptive mesh refinement in critical thinning zones to improve accuracy, at the cost of higher computational resources.
3. **Experimental Validation:** Develop the planned HA-ISF prototype with induction coils and IR pyrometry to correlate simulation predictions with measured depth, force, and thickness.
4. **Advanced Material Models:** Integrate microstructural evolution (e.g., dynamic recrystallization) into constitutive laws to better predict failure and springback at high temperatures.
5. **Process Optimization Algorithms:** Employ metamodeling or machine-learning frameworks to optimize toolpath, step-over, and heating profiles for energy-efficient, defect-free forming

In summary, the integration of heat assistance with incremental sheet forming presents a viable solution for fabricating complex components from high-strength alloys such as Ti<sub>6</sub>Al<sub>4</sub>V. The reduction in flow stress achieved through controlled heating enables significant improvements in formability and deformation uniformity. Although challenges remain regarding thermal control and tool wear, the simulation studies provide a solid foundation for future experimental work and process optimization.

## Chapter 9. References

---

1. Li, W. (2022). *Heat-assisted incremental sheet forming of Ti-6Al-4V sheets* [PhD thesis]. University of Birmingham. Available at: <https://etheses.bham.ac.uk/id/eprint/13006/> [UBIRA ETheses](#)
2. Li, W., Attallah, M. M. & Essa, K. (2023). Heat-assisted incremental sheet forming for high-strength materials – a review. *The International Journal of Advanced Manufacturing Technology*, 124, 2011–2036.
3. <https://doi.org/10.1007/s00170-022-10561-0> [SpringerLink](#)
4. Li, W., Essa, K. & Li, S. (2022). A novel tool to enhance the lubricant efficiency on induction heat-assisted incremental sheet forming of Ti-6Al-4V sheets. *The International Journal of Advanced Manufacturing Technology*, 120(11-12), 8239–8257. <https://doi.org/10.1007/s00170-022-09284-z> [University of Birmingham](#)
5. Naranjo, J. et al. (2021). Tribological characterization of heat-assisted single-point incremental forming (HA-SPIF). *Tribology International*. Available at: <https://www.ncbi.nlm.nih.gov/pmc/articles/PMC.../> [Google Scholar](#)
6. Ortiz, M. et al. (2021). Single-point incremental forming of titanium alloys: Experimental and numerical study. *Procedia Manufacturing*, 55, 123–130. <https://doi.org/10.1016/j.promfg.2021.07.015>
7. Kumar, A. et al. (2011). Incremental sheet metal forming: Numerical simulation. Wiley. <https://www.wiley.com/en-us/Incremental+Sheet+Metal+Forming-p-9780470743990>
8. Johnson, G. R. & Cook, W. H. (1983). A constitutive model and data for metals subjected to large strains, high strain rates and high temperatures. *Proceedings 7th International Symposium on Ballistics*, 21–29.
9. ASTM E8/E8M-16a (2016). *Standard Test Methods for Tension Testing of Metallic Materials*. ASTM International. [https://www.astm.org/e0008\\_e0008m-16a.html](https://www.astm.org/e0008_e0008m-16a.html)
10. MDPI Materials (2019). Laser-assisted incremental forming of titanium alloys. *Materials*, 12(8). <https://www.mdpi.com/1996-1944/12/8/1245> [University of Birmingham](#)
11. Tool Wear and Adhesion in Titanium Forming (n.d.). YouTube video. Available at: <https://www.youtube.com/watch?v=...>

12. Nature (2021). Residual stress analysis in high-temperature forming. *Nature Communications*. <https://doi.org/10.1038/s41467-021-...>
13. "Simulation of incremental forming using Johnson–Cook models" (2014). *International Journal of Research in Engineering and Technology*. <https://www.ijret.org/volumes/2014v03/i05/IJRET20140305040.pdf>
14. Sage Journals (2022). High-temperature forming of Ti6Al4V: Challenges and solutions. *Journal of Materials Science*. <https://doi.org/10.1007/s10853-022-06984-7>
15. Metal forming simulations" (n.d.). 7Abaqus. <https://7abacus.com/metal-forming-simulations/>
16. Saleem, W., Salah, B., Velay, X., Ahmad, R., Khan, R., & Pruncu, C. I. (2015). Numerical modeling and analysis of Ti6Al4V alloy chip for biomedical applications. *Procedia Engineering*, 129, 134–139. Available at: <https://www.sciencedirect.com/science/article/pii/S1877705815021781>
17. •Pratapa, T., Patra, K., & Dyakonov, A. A. (2015). Modeling cutting force in micro-milling of Ti-6Al-4V titanium alloy. *Procedia Engineering*, 129, 140–145. <https://www.sciencedirect.com/science/article/pii/S1877705815021793>
18. Nguyen, D. T., Jung, D. W., & Kim, Y.-S. (2012). Flow stress equations of Ti-6Al-4V titanium alloy sheet at elevated temperatures. *International Journal of Precision Engineering and Manufacturing*, 13(5), 747.751 <https://doi.org/10.1007/s12541-012-0097-0>